ISSN 1016-3115

wgn

30-1/2
february/april 2002

bimonthly journal of the international meteor organization

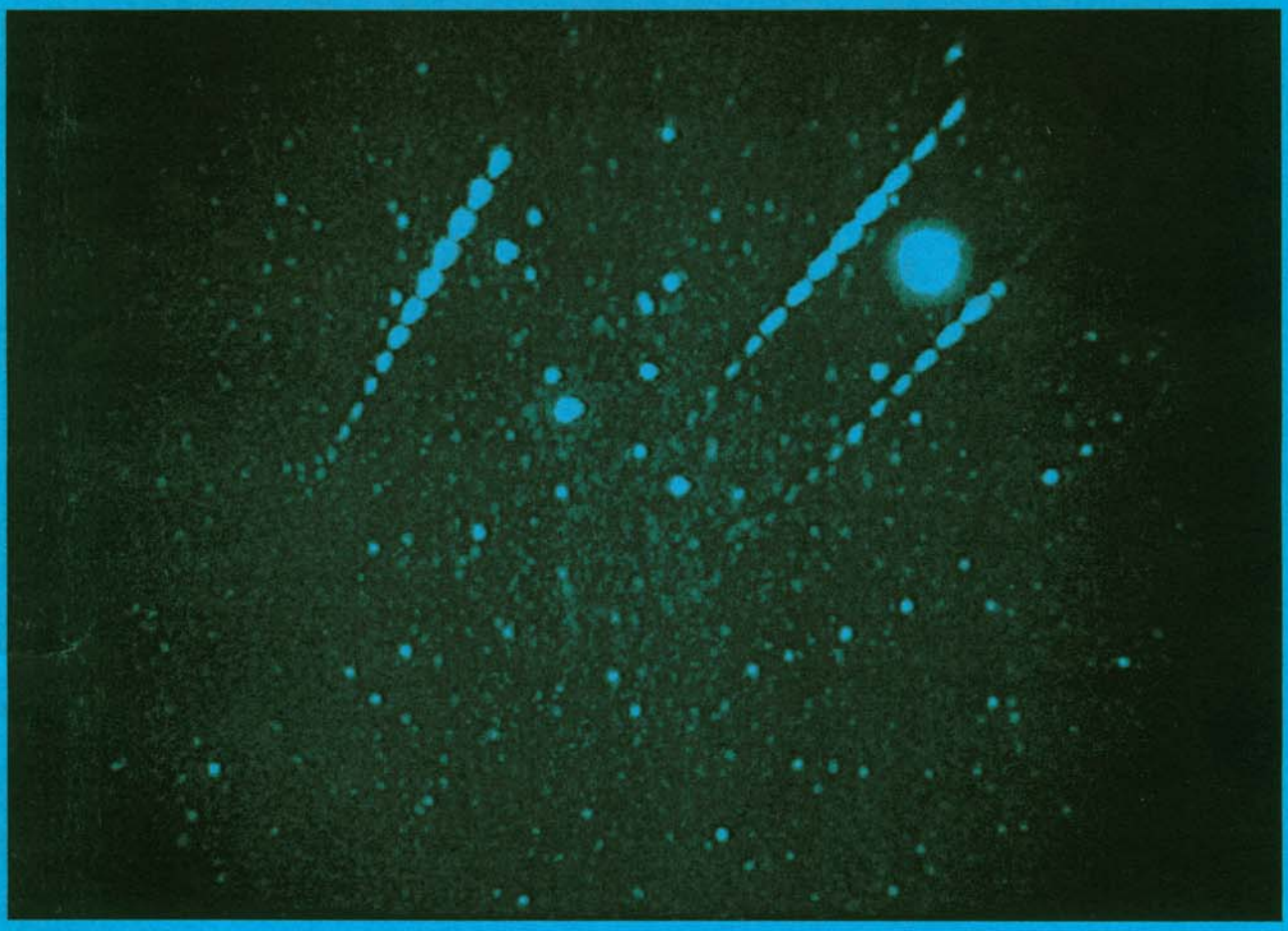

Among the most memorable experiences during meteor storms are those instances at which several meteors appear in the same second. In most cases, these meteors occur at some distance from one another, which is why they are rarely recorded by narrow-angle video cameras. *AKM* member Thomas Kurtz and colleagues observing with an image-intensified video camera from New Mexico, USA, however, were lucky when they captured a cluster of three bright meteors appearing only a few degrees apart at *exactly* the same time on November 18, 2001, $9^h42^m51^s$ UT. The exposure time of this image is only 0.8 s. The two bright stars above the center are Castor and Pollux, and up right, framed by two of the Leonids, is Jupiter. Details about the equipment and result from the analysis of this Leonid observation can be found elsewhere in this issue.

In this issue:

In case of non-delivery, return postage guaranteed. Please return to:
v.u.: Marc Gyssens, Heerbaan 74, B-2530 Boechout, Belgium

WGN, Vol. 30, No. 1/2,

February/April 2002, pp. 1–44

Contents

Useful Information

The June issue *(WGN 30:3)*

The *June issue* will be edited in the beginning of June 2002. Contributions should be sent as soon as possible to *Marc Gyssens*.

Subscriptions and ordering of publications

Volume 30 (2002) of *WGN* is expected to contain at least 240 pages and costs 20 EUR, including non-airmail delivery. Ordering other *IMO* publications is done in the same way as paying subscription/membership fees. Changes of address and complaints about not receiving *WGN* should be addressed to the Treasurer, Ina Rendtel.

All addresses can be found on the inside of the back cover.

The 2002 International Meteor Conference

Frombork, September 26–29, 2002

Mariusz Wiśniewski, Arkadiusz Olech, Marcin Gajos, Kamil Złoczewski, and Aleksander Trofimowicz

We have a great pleasure to invite you to Frombork—the city of Nicolaus Copernicus. The place for the *IMC* 2002 was not chosen accidentally. Frombork is the beautiful small town placed near the Vistula Bay with a nice view on the Vistula Sand-bar. The most important part of the town is the Cathedral Hill with many historical monuments including the Gothic cathedral, and the Copernicus tower, where the great astronomer was making his observations.

The 2002 *IMC* will take place in days September 26–29 and it will be organized by the Polish *Comets and Meteors Workshop (CMW)*. The *CMW* is an astronomical organization founded in 1987. Its main goal is to coordinate the comet and meteor observations in Poland. Since 1994 the *CMW* is one of the most active group of visual observers in the world.

The detailed information about getting to Frombork, the *IMC* hotel, the reduced fees and other important things are available at our web pages: `http://www.astrouw.edu.pl/~olech/pkim/imc2002/imc.html`. The registration fee including lodging, all meals, and the excursion is 100 EUR. We will provide bus transport from Gdańsk to Frombork. Please find the registration form for the Conference on page 2 of this issue. If you have any problems, questions, suggestions or requirements do not hesitate to contact

Mariusz Wiśniewski, ul. Afrykanska 10, 03-966 Warszawa, Poland,
e-mail: `pkim@astrouw.edu.pl`, phone: +48-22-672-38-81, mobile phone: +48-607-49-13-09.

The registration form should be returned to the Treasurer of the *IMO*,

Ina Rendtel, Mehlbeerenweg 5, D-14469 Potsdam, Germany,
e-mail: `treasurer@imo.net`, phone: +49-331-520-707.

Financial Support to Participants of the 2002 IMC

communicated by the IMO Council

As last year the *IMO* makes available funding to support attendance to the *2002 International Meteor Conference (IMC)*. If you wish to apply for support, proceed as follows:

1. E-mail your application to the *IMO* President, Jürgen Rendtel, at `president@imo.net`. The application must be submitted by an *IMO* member, but may also request support for other meteor workers of the same local, national meteor group as the *IMO* member. The proposal must state that all the candidates are committed to attend the *IMC* (except unforeseen circumstances) if the requested support is accorded in full.
2. An *IMC* Registration Form for each of the persons for which support is requested should be returned for the application to be valid, except if such a form was already sent earlier.
3. The application must also contain a brief curriculum vitae of each of these persons, focusing on aspects relevant to meteor work. Supported participants are expected to present either a talk or a poster at the *IMC* (to be indicated on the Registration Form).
4. The application must contain a motivation for attending the *IMC* and the importance of it to the person or group of persons requesting support.
5. The application must contain a budget for travel costs and registration, and the amount of support requested from the *IMO*. Other sources of external support, or their absence, must be mentioned. Finally, the proposal must also indicate to which extent *IMO* support is essential for being able to attend the *IMC*.
6. The applications should reach the President no later than June 15, 2002. The decision of the *IMO* Council will be made within two weeks after receipt of the application. If the requested support is accorded in full, the registration forms become final. If the requested support is not accorded, or only partially accorded, the candidates should inform the President within three weeks after notification of the *IMO* Council's decision if they want to sustain or withdraw their registration. The accorded support will be paid in cash at the *IMC*. Any unpaid registration fees will be deducted from the amount paid to the candidates.

We strongly encourage all meteor workers who are motivated to attend the *2002 IMC*, but who are prevented to do so by financial considerations, to make use of this opportunity and to apply for support. Information about this *IMC* can be found above.

International Meteor Conference

Frombork, Poland, September 26–29, 2002

Registration Form

Each individual participant should fill out a form and return it to *Ina Rendtel, Mehlbeerenweg 5, 14469 Potsdam, Germany*, as soon as possible. Your registration will be guaranteed only after Ina Rendtel has received the minimum pre-payment of 50 EUR. If you wish to participate, but cannot yet decide, simply return this form with the proper option checked to stay on the mailing list for further circulars.

Name: _____ Birth date: _____

Address: _____

_____

_____

Phone: _____ Fax: _____ E-Mail: _____

- ○ wishes to register for the 2002 *IMC* from September 26 to 29;
- ○ intends to participate, cannot yet register, but wishes to stay on the mailing list.

I intend to travel by _____, together with _____

Additional requests:

- ○ I need travel information from _____ to Frombork;
- ○ I wish to stay in Poland before or after the *IMC* and require additional information.

For participants wishing to contribute to the program:

Lecture: _____

Duration: _____min. Required equipment: _____

Workshop or discussion: _____

Poster presentation: _____ Space: _____ m^2

Either the entire fee of 100 EUR or a pre-payment of 50 EUR should be sent to the Treasurer, *Ina Rendtel*. Follow the payment instructions below. Participants making a pre-payment only have to pay the remaining 50 EUR in cash upon arrival in Frombork.

Date and signature: _____

Please send your payment to the Treasurer or one of her assistants as indicated below:

- in Europe: pay in EUR to Ina Rendtel, account number 547234107 at Postbank Berlin, bank code 10010010. No bank checks, please! (Bank checks can only be sent to Robert Lunsford, see below).
- in the UK: proceed as above or pay to Alastair McBeath, 12A Prior's Walk, Morpeth, Northumberland NE61 2RF, England.
- in Japan: pay to Masahiro Koseki, 4-3-5 Annaka, Annaka-shi, 379-01 Gunma-ken, Japan.
- all others pay in USD to Robert Lunsford, 161 Vance Street, Chula Vista, California 91910, USA. In case you pay by bank check, make it payable to Robert Lunsford, *not* the *IMO*!

People wishing to pay in other currencies should contact the appropriate IMO *contact person for exchange rates.*

Leonids

Comparison of the "American" and the "Asian" 2001 Leonid Meteor Storm

Sirko Molau, Peter S. Gural, and Osamu Okamura

Leonid activity profiles obtained from one airborne and two ground- based intensified video cameras, which observed both peaks of the 2001 Leonid meteor storm, are analyzed. After corrections for the topocentric time of the stream encounter, radiant altitude, and detection efficiency of the camera systems, we find that the Asian storm peak caused by the 4-revolution dust trail occurred at 18^h14^m UT. It reached 2.3 times the level of activity of the two American peaks caused by the 7-revolution trail with maxima at 10^h43^m and 11^h02^m UT. The airborne data set indicates an earlier second Asian peak at 17^h39^m UT, but to link this peak to the passage of the 9-revolution trail is questionable. Whereas the peak times and the peak activity ratio between both storms agree well with the global analysis of visual observations, we find a much lower population index on the order of $r = 1.35$ for faint meteors.

1. Introduction

Numerous observers worldwide eagerly awaited the 2001 Leonid maximum, as it was predicted to become the most impressive Leonid display of the current perihelion passage. These predictions had been based on models developed subsequent to the unexpected "fireball night" of 1998. By that time, theorists re-introduced the dust trail model (Asher 1999; McNaught & Asher 1999) originally proposed by Kondrat'eva & Reznikov (1985) to help explain the observed 1998 Leonid activity and predict future encounter conditions. The model's central concept is that meteoroids are not concentrated strictly along the current orbit of the comet, but that there are several distinct dust trails. Each trail was produced at one of the previous perihelion passages of parent comet Tempel-Tuttle. Since the comet undergoes gravitational perturbations and accelerations from other dynamical forces such as dust and gas emission, it's orbit changes with time. Thus, the original dust trails are slightly displaced from revolution to revolution and are later gravitationally perturbed and affected by solar radiation pressure once ejected from the comet. To predict meteor storms one must evaluate how close the Earth comes to each of these trails and at what time the closest approach takes place.

The dust trail model was highly successful in predicting the 1999 Leonid storm to within an accuracy of five minutes, but the predicted ZHR was off by almost one order of magnitude (Arlt et al. 1999). This is only natural, since the time of passage of the Earth through the meteoroid stream can be much more accurately calculated than the meteoroid density distribution within and along the trail. In 2000, however, the differences between the predicted and observed activity peak times were up to 40 minutes (Arlt & Gyssens 2000). Compared to the "pre dust trail era" the forecast was still amazingly accurate, but a little worse than anticipated after the almost perfect match in 1999. The predicted maximum ZHR in 2000 was again two to five times off, with the model of Lyytinen & van Flandern (1999) producing results closest to the observations.

Early predictions for the 2001 maxima were quite uniform. McNaught and Asher (2001) as well as Lyytinen, Nissinen and van Flandern (2001) identified three dust trails as the main contributors to Leonid activity, namely the 7-, 9-, and 4-revolution old trails. However, when looking over the predictions in greater detail, the forecasted peak times of both groups differed by up to 30 min (see Table 1). With respect to the peak ZHR both models agreed that the Asian peak, which actually consisted of two nearby maxima caused by the 9- and 4-revolution trails, would outperform the 7-revolution trail American peak significantly. Whereas the American maximum was expected to be near the limits of a meteor storm, the composite Asian maximum was predicted to be even stronger than the 1999 Leonid storm.

In the model by McNaught and Asher, meteoroid orbits are only influenced by gravitational forces and solar radiation pressure. The model of Lyytinen et al., however, includes additional non-gravitational perturbations such as the Yarkovsky effect. These extra perturbations cause a shift in peak times relative to the McNaught and Asher model. Hence, the 2001 encounter was not only a good test for the dust trail theories in general, but also for determining the importance of non-gravitational forces on dust trail orbital perturbations.

The picture became somewhat confusing when Jenniskens presented a talk at the Meteoroid 2001 conference in Kiruna during August 2001. Based on the first two dust trail models, he predicted that the American peak would be several times stronger than the Asian peak (Jenniskens 2001a). Jenniskens explained this by a small shift of the dust trails perpendicular to the Earth's orbit he found in Leonid observations of the previous years. Even though Jenniskens later scaled down his initial activity figures significantly, he still forecasted main activity over America with much weaker individual peaks over Asia (Jenniskens 2001b). Thus, a comparison of the relative strength of American to Asian peaks would aid in judging the reality of the dust trail shift model (note that the merged Asian peaks were expected to have a fluence similar to the single American peak).

Finally there was the model of Brown and Cooke (2001), which in contrast to the dust trail models did not predict sharp peaks close to the trail encounters, but a broad activity plateau reaching storm level at maximum between 12^h00^m and 13^h00^m UT. It results from extensive 3-dimensional particle simulations, but some basic model assumptions or parameters need re-examination, as the predicted activity profiles had only little in common with the observed one.

Table 1 – Dust trail model based predictions for the 2001 Leonid storms by different theorists (adapted from McNaught & Asher 2001, Lyytinen et al. 2001, and Jenniskens 2001b) and results obtained from video observations described in this paper.

Dust	McNaught/Asher		Lyytinen et al.		Jenniskens		Video Observation		
Trail	UT	ZHR	UT	ZHR	UT	ZHR	UT	ZHR	FWHM
7-rev	09^h55^m	800	10^h28^m	2000	10^h09^m	4200	10^h43^m, 11^h02^m	ZHR_{Am}	108 min
9-rev	17^h24^m	2000	18^h03^m	2600	17^h08^m	1800			
4-rev	18^h13^m	8000	18^h20^m	5000	17^h55^m	2700	18^h14^m	$2.3 \times ZHR_{Am}$	109 min

2. Leonid observations 2001

Due to the large temporal separation of the two predicted Leonid peaks in 2001, it was impossible for a ground-based observer to record both maxima unless he was situated near the north geographic pole (a place where the weather is highly unfavorable for visual/video observations and local support infrastructure is lacking). However, thanks to hundreds of visual meteor observers world-wide sending in their data to the *IMO*, it was possible to derive a detailed ZHR profile across both maxima. In their global analysis of the visual data, Arlt et al. (2001) found ZHR peaks of about 1600 at 10^h39^m and 11^h03^m UT for the American storm, and a peak ZHR of about 3700 at 18^h16^m UT for the Asian storm, i.e. a peak ratio of 1:2.3. Contrary to previous year's analysis however, the peak ZHR (especially of the 7-rev trail) has changed significantly during the intermediate analysis stages. It was found that a few observers with exceptional perception may have severely influenced the derived activity profile.

Image-intensified video systems are much less prone to observational errors. Their meteor detection probability is fixed for the whole observing period given that the observing conditions and geometry (limiting magnitude, radiant position, and pointing direction) remain the same.

However, there were far fewer video systems in operation than visual observers, and a ground-based video system's counting statistics are typically worse (i.e. they record fewer meteors than visual observers for a given interval of time). In addition, the camera parameters vary much more widely from one system to the next compared to human observers. That is, for any given camera one is able to derive a detailed activity profile, but the comparison of the relative strength of the two Leonid peaks from recordings of different video systems is difficult.

For these reasons we concentrate here on two special data sets that were obtained by ground-based German video teams and an airborne Japanese video observation. The aim is to compare the relative strength of both Leonid peaks and to estimate the peak times from these data. A more thorough analysis to refine the peak times and concentrate on fine structures within the activity profile, using data from other video systems, will follow in a future paper.

3. The German data set: Observation and analysis

The German Arbeitskreis Meteore working group owns two identical image intensified meteor cameras, AKM I and AKM II. Each system consists of a 25mm, f/0.85 c-mount lens, a second-generation Delft Photonics image intensifier with 18 mm photo cathode, and a CCD video camera. The cameras have a field of view of 32 deg and a typical limiting magnitude for stars beyond 7th mag. AKM I was operated by Thomas Kurtz and colleagues from New Mexico, USA, and recorded the American Leonid storm between 5^h36^m and 12^h42^m UT. Jan Hattenbach and Georg Görgen from the public observatory Aachen operated the twin camera AKM II near the city of Lindian, China. The second camera completely covered the Asian peak during its operation from 14^h37^m to 21^h45^m UT. The video streams were recorded at both sites in PAL format on VHS tape and later analyzed by Sirko Molau.

The first step was to scan the tapes for meteors using the MetRec automated meteor detection software (Molau 2001). In the American data, a total of 361 meteors were detected in 6.9 hours of effective observing time, 196 of which were identified as Leonids. The tapes of the Asian camera contained a total of 715 meteors including 594 Leonids, recorded in 7.1 hours effective observing time. Already these initial figures indicated that the Asian storm had clearly outperformed the American storm both in peak activity and duration, given that the observing conditions were comparable.

A second manual review of the most important sections of the video tapes (AKM I: 9^h30^m–12^h00^m UT; AKM II: 17^h00^m–20^h00^m UT) was carried out in order to increase the meteor detection probability, refine the shower association, and avoid systematic errors and selection effects possibly introduced by the software. As it turned out, MetRec had an overall detection rate of 75% (83% for Leonids) on the American and about 81% (82% for Leonids) on the Asian data. Most of the meteors not detected by the software were very faint. Those few cases where brighter Leonids were missed was because (1) they appeared in very short succession of one another, (2) they appeared parallel to a very bright meteor, or (3) they occurred near the edge of the field of view (note that MetRec can detect meteors appearing at the same time, but there is a short dead time of less than one second every time a meteor image is saved to disc). There was no indication that the detection probability depended on the apparent angular velocity of the meteor. This is important since the American camera was pointed in close proximity to the radiant. The meteor shower assignment was found to be in error for only a few cases associated with very bright meteors, situations where the meteor position and direction could not be determined accurately by the MetRec software due to blooming and saturation.

Using the manually verified meteor counts (AKM I: 288 meteors including 169 Leonids between 9^h30^m and 12^h00^m UT; AKM II: 626 meteors including 532 Leonids between 17^h00^m and 20^h00^m UT), an activity profile versus time was plotted (Figure 1). Leonid counts were computed in 5-minute bins with a 2.5-minute shift. They were corrected for both the topocentric time of the stream encounter and the increasing radiant altitude.

For the American camera, we find two weak maxima at 10^h43^m and 11^h00^m UT. The second camera situated in Asia shows a strong peak at 18^h13^m UT which is about three times as high, and a number of secondary maxima before and after the peak. However, none of these can clearly be attributed to the 9-rev trail. As a consistency check we plotted the number of all non-Leonids (Taurids, alpha-Monocerotids, and sporadic meteors) that should show an approximately even flux profile over the two observation windows. They were averaged in 20-minute bins with a 10-minute shift. Here the American camera shows slightly higher values than its Asian counterpart (48 versus 31 meteors per hour on average).

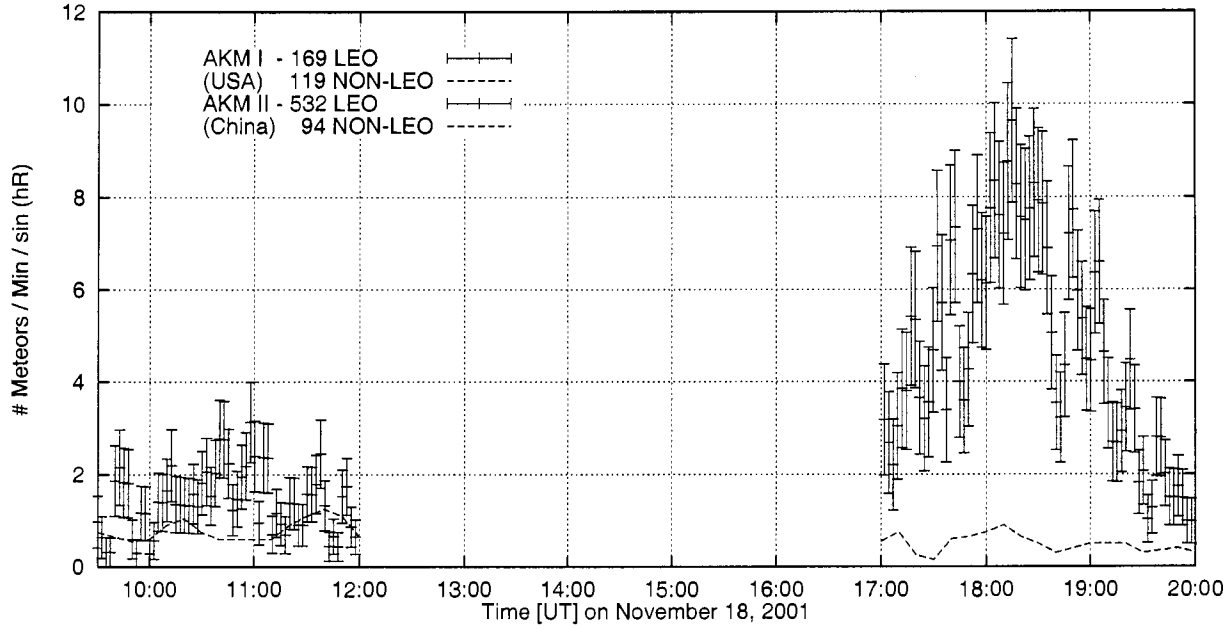

Figure 1 – Leonid activity curves for the two German cameras AKM I and II. Leonid counts are corrected for the topocentric time of the stream encounter and the radiant altitude. They are averaged in 5 min bins with 2.5 min shift, error bars are given for $\sqrt{n_{\mathrm{LEO}}}$. Non-Leonids are uncorrected and averaged in 20 min bins with 10 min shift.

4. The Japanese data set: Observation and analysis

Japanese amateur Osamu Okamura is one of the few and perhaps the only observer who managed to witness both Leonid peaks. He booked a flight from Los Angeles, USA to Taipei, Taiwan and mounted three image-intensified meteor cameras behind windows in the second floor of the Boeing 747 pointing generally in the northern and southern directions. The cameras were equipped with 50-mm $f/1.2$, 28-mm $f/1.4$ and 35-mm $f/2.0$ photographic lenses, second-generation image intensifiers, and three digital NTSC video cameras. A black cloth was glued around the equipment and window to avoid focusing problems and stray light reflections, a lesson that was learned during his 1998 and 1999 airborne observations.

Due to technical problems, only the first two cameras could be operated. Still it was a busy night for Okamura, as he had to operate the cameras, change the tapes, record the airplane's position by GPS, replace batteries and explain to his neighbors what he was doing. Here we concentrate on the data set collected with the 28-mm wide-angle camera with a nominal field of view of 45 degrees in diameter and a limiting magnitude close to +7 mag. Meteor activity was monitored continuously between 8^h45^m to 20^h37^m UT from an altitude of about 9500 m. There were time intervals of reduced detection performance when the airplane went through clouds or changed it's flight direction (9^h04^m–9^h26^m, 11^h03^m–11^h20^m, 11^h26^m–11^h44^m, and 11^h50^m–12^h43^m UT), but in general the derived activity profile is complete for almost 11.2 hours of effective observing time.

Back home Okamura inspected his video tapes manually. Overall a total of 8744 meteors including 8353 Leonids were found. Thanks to the reduced atmospheric extinction of the 9.5 km high "observing site", the airborne camera recorded many more meteors than the ground-based systems, an effect which was previously noted during both the 1998 and 1999 Leonid-MAC campaigns (Koschny & Zender 2000; Gural & Jenniskens 2000). The aircraft's position was recorded every 30 minutes in order to later compute the radiant position and relative camera pointing. Meteor counts were corrected for the topocentric stream encounter time and the radiant altitude and binned in 5-minute intervals with a 2.5-minute shift. Non-Leonids were averaged in 20-minute bins with a 10-minute shift.

The airborne data reveal two activity maxima for the American storm at $10^{h}43^{m}$ and $11^{h}05^{m}$ UT. Whereas the first peak coincides perfectly with the ground-based video data of AKM I, there is a minor offset of 5 minutes for the second peak. The main Asian peak at $18^{h}15^{m}$ UT matches again the time of peak activity in the data collected with AKM II. There is a clear secondary peak at $17^{h}39^{m}$ UT which could be a manifestation of the 9-revolution dust trail (a time at which we find enhanced activity in the ground-based camera data as well), and a third period of heightened activity between $18^{h}31^{m}$ and $18^{h}37^{m}$ UT. Note that for this data set the Asian storm peak outperforms the American peak only by a factor two.

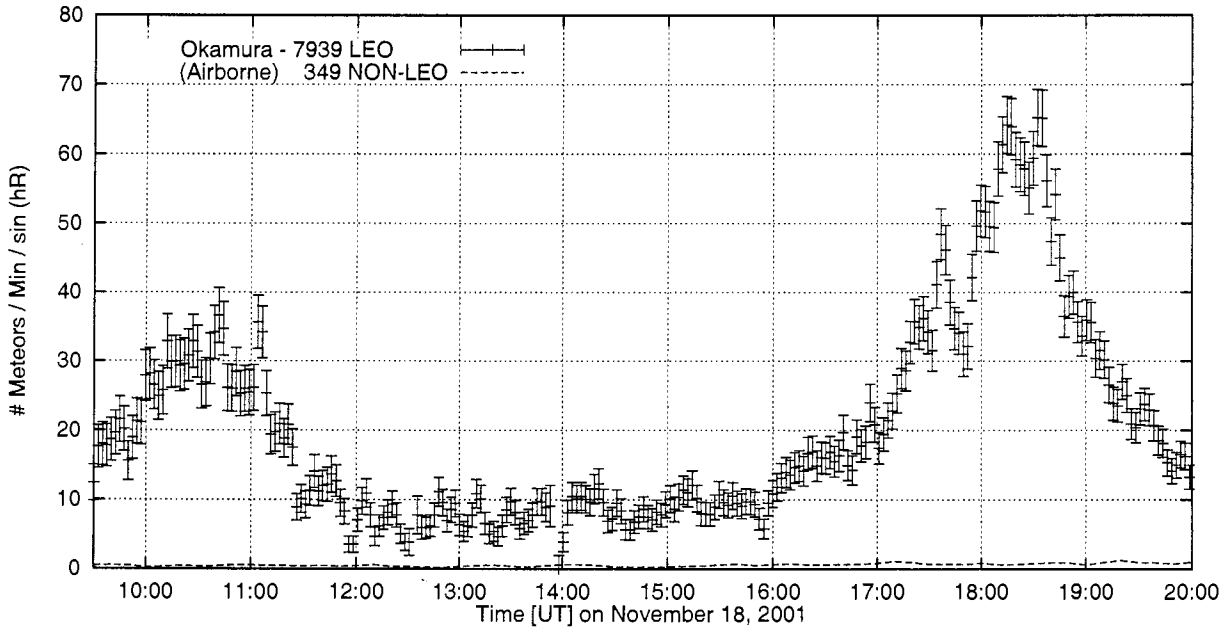

Figure 2 – Leonid activity curve for the Japanese airborne data. Leonid counts are corrected for the topocentric time of the stream encounter and the radiant altitude. They are averaged in 5-min bins with 2.5 min shift, error bars are given for $\sqrt{n_{\mathrm{LEO}}}$. Non-Leonids are uncorrected and averaged in 20 min bins with 10 min shift.

5. Issues to be addressed through simulation and analysis

In the following sections we discuss and account for a number of effects that have influenced the derived Leonid counts in a systematic way so as to obtain a more accurate measure of the peak flux ratio. These include the impact of pointing direction differences between cameras, differences in the camera operational specifications, changes in the limiting magnitude between cameras and with time, and the influence of the population index of the Leonid stream at the times of encounter.

The twin AKM cameras were identically constructed and equipped, but still did not match each other exactly in observing conditions and pointing directions. To determine the limiting magnitude for both cameras at their respective observing sites, we integrated 16 video frames

for each of them and determined the faintest visible stars (ignoring very red and blue ones). For the American camera, the limiting stellar magnitude was found to be about +8.2 mag near the center. Due to vignetting it falls off near the edges to about +7.5 mag. The values are slightly worse for the Asian camera (+7.7 and +7.0 mag, respectively) because it was not perfectly focused. In single video frames the limiting stellar magnitude was found to be about 1.5 mag lower due to the lower signal-to-noise ratio. If we account for the differences in limiting magnitude between cameras, the American Leonid peak becomes relatively weaker compared to the Asian, but the non-Leonid counts match more closely.

The observing fields of the two AKM cameras were also not synchronized. During the observation AKM I was pointed at an azimuth of 109°.5 and elevation of 70°.5, whereas AKM II was pointed at an azimuth of 220°.5 and elevation of 44°.5. That is, for the most interesting period between 9^h30^m and 12^h00^m UT, the distance between the Leonid radiant and the American camera's field of view (FOV) center decreased from 35°.4 to 3°.6. Between 17^h00^m and 20^h00^m UT the Asian camera was pointed at a much larger radiant distance varying between 98°.9 and 57°.5 over the period of the observation and much lower in elevation angle.

For the airborne camera, the limiting magnitude was derived by comparison of the live video image with a star map excluding red and blue stars. It varied between +5.7 and +6.9 mag. However, near the time of the two major peaks it was almost a constant +6.8 mag for stars. The camera was pointed at a nominal 29° elevation but the azimuth and the angular distance to the radiant varied as a function of time. This was due to the steadily shifting flight orientation and geo-spatial position as the aircraft followed a great circle route from Los Angeles to Taipei.

The effect of different observing directions can hardly be estimated or analytically derived, as it depends on many parameters. On the one hand, larger radiant distances cause an increase in apparent angular Leonid velocity, which will result in an effective reduction of the camera's limiting meteor magnitude. On the other hand, meteor trails are longer at larger radiant distances giving them a higher probability to cross a camera's field of view. A camera pointed at lower elevation will monitor a larger atmospheric volume with increasing extinction. In which way meteor counts are influenced by these effects depends heavily on the population index, i.e. the percentage of bright meteors in the stream's magnitude distribution.

We decided to use a meteor simulation software tool developed by Peter Gural to derive time-dependent Leonid detection efficiencies for each camera and apply corrections to the observed activity profiles. The remaining difference in counting levels should be attributable to the relative flux ratio of the two Leonid peaks given that the detection efficiency of the humans and computer software used to obtain the measured counts are constant.

6. Meteor simulation tool

The simulation tool MeteorSim was first described in Gural and Jenniskens (2000) and more recently in Gural (2001). Details of the formulations can be found therein. The program can be described as a Monte Carlo simulation whereby a randomly positioned meteoroid is placed outside the Earth's gravitational sphere of influence and propagated along a specified radiant direction. The meteoroid is acted on only by the Earth's gravity (geocentric flight dynamics) yielding a hyperbolic orbit. The meteoroids are initially distributed in space in a three-dimensionally uniformly random pattern and initially move along parallel trajectories aligned with the radiant vector and possess identical velocities. Computations proceed by solving for the meteor's position at any point along the trajectory given the height above the mean Earth radius. From that position, the azimuth and elevation of the meteor from the observer or sensor can be computed. The particles are assumed to have a user specified population index r with particles ranging in brightness from -8.0 to $+7.0$ with the total number of particles in that magnitude range fixed. Magnitude losses for distance fading, extinction, and effective angular velocity across the CCD pixels is also accounted for as a function of look direction and meteor stream parameters.

The simulation run parameters for the three cameras are listed in Table 2. The FOV for both AKM cameras was a circular region equally cut off top and bottom by the rectangular CCD chip shape. The cameras were assumed to be oriented so that the flat edges of the FOV were aligned with the local horizon. The cameras recorded the sky imagery with an effective spatial resolution given by the FOV, the number of pixels across the frame and temporal integration time based on the interleave period for PAL and NTSC video. The limiting magnitudes are based on single frame stellar magnitudes with additional losses computed during runtime execution for each individual meteor's apparent angular velocity, distance from observer, and extinction. The Leonids were modeled with a radiant position for November 18, 2001, of $\alpha = 153\overset{\circ}{.}2$ and $\delta = +22°$, velocity at infinity of 71.3 km/sec, and begin/end heights of 108/95 kilometers. We initially adopted a population index of $r = 2.1$ for the 2001 Leonid peaks as derived from visual observations (Arlt et al. 2001). Note that for the American camera AKM I, the FOV includes the radiant towards the end of the observation period. This has a profound impact on the counts versus time due to the slower nature of meteors near the radiant and longer integration time a meteor sits on a given CCD pixel.

Table 2 – Camera run-time parameters used in the simulation.

Camera	AKM I (America)	AKM II (Asia)	Airborne
Location	33°.5 N / 105°.69 W	47°.2 N / 124°.9 E	27° ... 58° N / 123° W ... 124° E
Pointing center [azim./alt.]	109°.5 / 70°.5	220°.5 / 44°.5	322° to 45° / 29° nominally
Diameter of field of view	32° circular 26° cutoff	32° circular 26° cutoff	45° circular
Spatial resolution [arc min/pixel]	3.05	3.05	6.1 to 7.0
Integration time [s]	0.02	0.02	0.0167
Stellar limiting magnitude [mag]	+6.7	+6.2	+5.7 to +6.9
Nominal magnitude losses [mag]			
Difference from +6.5	+0.2	−0.3	−0.8 to +0.4
Extinction	−0.01	−0.09	−0.10
Distance to meteor	−0.16	−0.81	−1.4
Angular velocity	−2.16	−2.58	−1.2 to −1.7
Total losses	−2.13	−3.78	−2.8 to −3.5

Each simulation was run with 10 million initial particles for a fixed flux density of one meteoroid per square kilometer per unit of time. In agreement with the analysis of the video observations a simulation count was recorded for a given camera if a part of the meteor appeared anywhere in the FOV and if its magnitude was above the sensor's limiting magnitude after all losses were accounted for. Thus, the detection efficiencies will adjust the observed activity level for radiant altitude, apparent angular velocity, and meteor distance. The corrected meteor counts presented should be viewed in terms of relative flux levels between the two cameras or for the same camera over time, and not in terms of their absolute counts. To obtain detection efficiencies the simulation was run given the best estimate of each camera's specifications with some parameters varying with time (Table 2). The computed counts were divided by an "optimal" reference count determined for the same camera but pointed at the zenith with radiant at the zenith and a limiting magnitude of +6.5 mag. In subsequent analyses in this paper, these detection efficiencies were applied to measured raw counts from the video observations. We do not have to correct for radiant altitude beforehand since the detection efficiency has the correction implicitly included.

7. Initial simulation results for $r = 2.1$

The initial simulations showed several interesting features. From a sheer detection efficiency perspective, the ground-based American camera could see nearly 1.6 magnitudes deeper than its Asian counterpart just due to pointing differences relative to the radiant (see losses in Table 2). The Asian camera has an almost constant detection efficiency with time as expected for a camera pointed away from the radiant. The counts for the American camera, on the contrary, are seriously influenced by the changing dwell time of a meteor within a given pixel (apparent angular velocity). During the 2.5 hours of interest its detection efficiency was found to increase by a factor of three as the radiant entered the field of view (for $r = 2.1$). At the times of the observed peaks the American camera was capable of detecting 75% more meteors per unit time than its Asian twin, which increases the peak ratio to an unreasonably large factor of almost six according to the given setup.

The Japanese camera, on the other hand, shows a 25% decrease in detection efficiency at the time of the second peak, which results in a corrected peak activity ratio of about 2.5. During the middle of its observation period the efficiency drops due to decreasing limiting magnitude at that time, but both peaks in the activity profile occurred when the Japanese camera was operating near a limiting magnitude of +6.8 mag.

To explain the discrepancy in both data sets and especially the unreasonable large peak ratio for the ground-based cameras, we studied possible error sources of the video data analysis and what systematic effect they may have:

- **Statistics:** The figures we derived for the Asian peak are more accurate than for the American peak. This has several reasons. First there were significantly more Leonid meteors observed over Asia, which provides better statistics. At the peak time in Asia, both the ground-based and the airborne camera observed in a direction with only minor changes in detection efficiency over time. Consequently, the shape of the ground-based and airborne activity profiles as well as the peak time agree well. At the time of the American storm, the opposite was true, both camera field centers were located such that the detection efficiency changed significantly over time. Even at the peak the ground-based camera recorded on average only two Leonids per minute, which results in large error bars. The accuracy of the airborne data was also reduced at that time due to interference from the acquisition light on the right side of the aircraft. So it comes as no surprise that ground-based and airborne activity profiles of the American storm differ by a greater extent, but this difference cannot explain the large discrepancies in the peak ratios after correction for each camera's detection efficiency.
- **Limiting magnitude and FOV:** The limiting magnitude and the diameter of the field of view of a video camera are crucial numbers when it comes to meteor detection efficiency. Contrary to visual observers, we know the diameter of a video system's FOV with high accuracy. Also the observing direction and radiant distance are precisely known at any point in time. As the Asian AKM camera was slightly out of focus, we measured a degradation of stellar limiting magnitude by 0.5 mag compared to the American counterpart. This is in good agreement with the observed 50% excess of non-Leonid meteors in the American camera data.
- **Slow versus fast meteors:** Contrary to visual observers, the detection probability for meteors is independent of the meteor location within the field of view neglecting small losses for vignetting. However, one may argue that low velocity meteors are more difficult to detect for both the software and the human observer, which would systematically lower the counts for a FOV close to the radiant. To evaluate this effect we computed a histogram of Leonids counts versus the distance of their starting point from the radiant for the American camera AKM I. We found no significant deviation from the same histogram derived for simulated meteors. Short and slow Leonids near the radiant were detected with the same probability as fast ones at greater distances. There is some loss within three degrees of the radiant but

for geometric reasons the counts are so low in that region that they amount to less than 3% of the overall meteor count in the FOV.

- **All Leonids versus Leonids with end points inside the FOV only:** Meteor trails are short near the radiant and long at large angular distances. In our analysis of the videotapes we included all visible Leonids, as this number was easiest to derive from the observations. One could argue that this is a bad choice, as the apparent length of the Leonid trails depends on the radiant distance and the altitude of the begin and end point which is not exactly known. The longer trail lengths can increase the effective viewing area of the camera when all meteors are used as a selection criteria. The simulation thus was set up to mimic the various possible selection criteria for meteors. It was found that the detection efficiency was only marginally affected by the meteor selection criterion.

In short, none of these effects could possibly have a large enough impact on the analysis to account for the discrepancies in flux ratio we observed in the data sets.

8. Population index

In the initial simulations we had assumed a population index of $r = 2.1$. Follow-up simulations with different population indices revealed that the detection efficiency ratio between two cameras looking in different directions is very sensitive to this parameter. Thus the question was raised as to whether the population index was incorrectly chosen and was the root cause of the flux ratio discrepancy.

In a previous analysis of the 1999 Leonids by Gural and Jenniskens (2000), the meteor simulation tool had been used to obtain an estimate of the population index independent of visual observer reports. This was done using the meteor counts from several different elevation angles measured with the same video camera (essentially changing the pointing direction for fixed incident flux, fixed camera detection efficiency, and fixed limiting magnitude). The steepness of the measured counts curve versus elevation angle was found to vary with the population index of the meteoroid stream and does not require an estimate of each individual meteor's magnitude. It does require high numbers of counted meteors, though, which were available in the 1999 Leonid MAC airborne data set.

By extension, it is possible to derive the population index from the flux ratio of two identical cameras observing at the *same time* and *same site* but pointed in two different directions. They would both experience the same incident flux and the simulation tool could remove the effects of different pointing directions. Hawkes (1998) had a similar idea for population index determination. He proposed to use two different f-stop settings on identical systems pointing in the *same direction* (same site and same time) with resultant different limiting magnitudes from which a count ratio would yield the population index. However, using the different pointing direction approach permits both cameras to operate at their peak detection efficiency to maximize statistics.

The situation with the data set investigated here is further complicated by the fact that identical cameras were operated at different times and locations. We cannot apply the same methodology indicated above, as both the relative activity level and the population index are unknown. However, we can still derive the detection efficiency of all cameras as a function of the population index and examine its impact on the flux ratio. The ground-based and airborne measurements can also be treated as independent data sets. The fact that they have vastly different dependencies on the r-factor is used to advantage in the subsequent analysis to determine both the population index and peak flux ratio for the 2001 Leonid storms.

The following discussion is based on the simulated detection efficiencies (Figure 3) of the three cameras at the times of peak flux ($10^{\mathrm{h}}45^{\mathrm{m}}$ and $18^{\mathrm{h}}15^{\mathrm{m}}$ UT). It turns out that the efficiency of the American camera AKM I observing close to the radiant is only lightly affected by the population index. Under the observing geometry of the American peak at 10:45 UT, the efficiency varies only by a factor of 1.5 in the population index range from 1.1 to 3.0. On the contrary, the

efficiency of the Asian camera AKM II depends heavily on the population index. Given the observing geometry at 18^h15^m UT we find efficiency variations by a factor of 15 (!) in the same population index range.

The efficiency of the airborne camera depends strongly on the population index as well, but here the variations are similar for both the American and the Asian peak. Given the 10^h45^m UT observing geometry, the detection efficiency varies by a factor 10, and under the observing conditions at 18^h45^m UT by a factor of 14 in the same population index range.

The reason for the different behavior of the cameras is the increase of apparent angular velocity at larger radiant distances, which results in a reduction of the limiting meteor magnitude. A stream with a high population index is dominated by faint meteors. They are easily missed at large radiant distances due to the reduced limiting magnitude. As the population index lowers, the stream is dominated by a greater percentage of bright meteors, which remain visible even with a greater loss in limiting magnitude due to high angular velocity. Hence, the detection efficiency of a camera observing far from the radiant increases rapidly with lower population indices. Near the radiant the apparent angular velocities are much lower. This results in a smaller decrease of limiting meteor magnitude, and variations in the population index are less important

What is significant to note in Figure 3 is that the *ratio* of detection efficiencies (at the peak times) is only weakly dependent on population index for the airborne camera, but it is strongly dependent for the ground-based. Thus the corrected flux count ratios of airborne and ground measurements versus r-factor will have different slopes and the conjecture is that where they cross would yield the desired information.

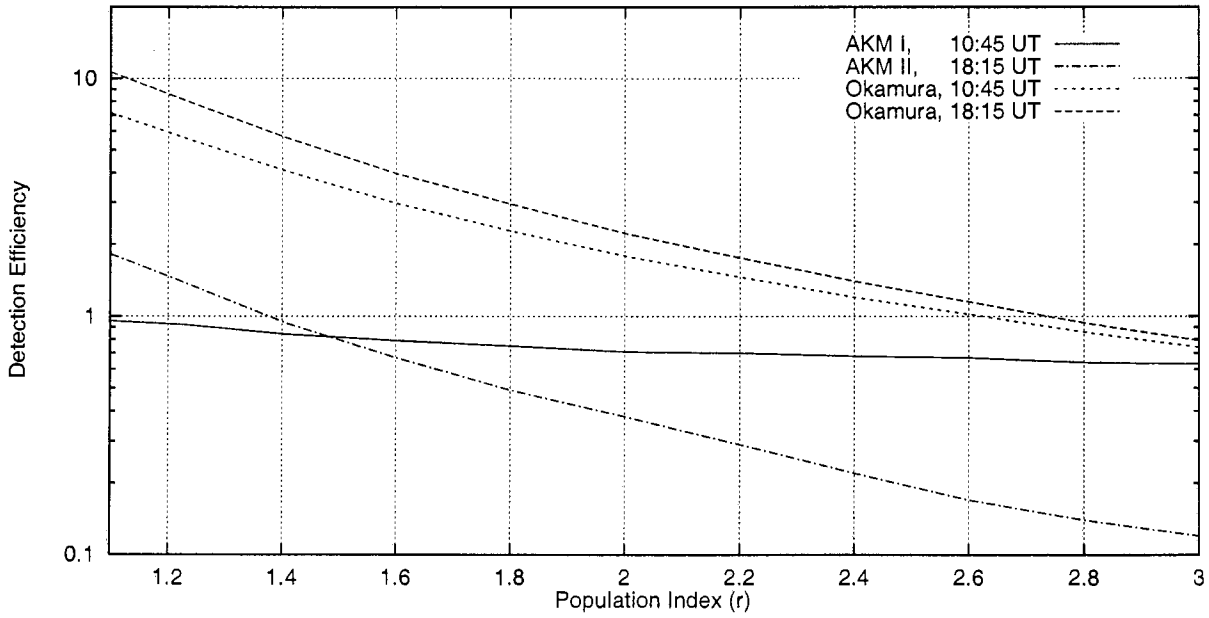

Figure 3 – Simulated detection efficiencies versus population index r for the three cameras at the times of peak flux. Note the strong dependency on r for those cameras pointed away from the radiant (logarithmic ordinate!) as opposed to the relatively flat response of camera AKM I observing close to the radiant.

To do this estimation with some level of error analysis, we re-derived the peak Leonid counts (n_{LEO}) per minute and applied a $\sqrt{n_{\mathrm{LEO}}}$ standard deviation to all the video measurements. Statistical errors in the detection efficiencies introduced by the large but finite number of meteors in the simulation, were much smaller than the measurement errors and were thus neglected. To average out short-term fluctuations and get a reliable estimate of the true peak activity, the counts were obtained from smoothed and over-sampled activity profiles (20 min bin size with

1 min shift). The peak counts (1.80 ± 0.29 Leonids/min for the American and 5.03 ± 0.49 Leonids/min for the Asian ground-based camera) were divided by the detection efficiency to derive normalized peak counts over r.

Next we calculated the ratio of both normalized peak counts as a function of the population index r under the assumption that r was the same for both peaks (as indicated in the visual record). If the peak fluxes were exactly known, we could just divide the values. In practice, however, we only know the values within certain error bounds. We assumed that the peak activities are normal-distributed measurements with the means and standard deviations given above. For large numbers, the ratio of two uncorrelated normal distributions with means μ_1, μ_2 and variances σ_1^2, σ_2^2 converges to a new normal distribution with mean $\mu = \mu_1/\mu_2$ and variance $\sigma^2 \approx \mu^2 (\sigma_1^2/\mu_1^2 + \sigma_2^2/\mu_2^2)$ (cf. the chapter on error propagation in Bevington, 1969). As we are dealing with small numbers here, the resulting distribution deviates from a normal distribution and the formulae become inaccurate. For this reason we determined the expectation value μ and variance σ^2 numerically. The normalized peak ratio for the two ground-based cameras over r is depicted in Figure 4 together with upper and lower bounds given by the standard deviation. For $r = 2.1$ we find a large peak ratio of six for the ground cameras as in our initial simulations, but for smaller population indices this ratio drops dramatically.

The same process was repeated for the airborne camera at the two peak times. Dividing the peak activity meteor counts of the camera (14.15 ± 0.82 Leonids/min for the American peak and 45.79 ± 1.45 Leonids/min for the Asian peak) by the detection efficiencies over r results in a second graph with upper and lower bounds (Figure 4). Since the detection efficiency at both peaks behaves similar for this camera over a large range of r-values, the Leonid peak ratio depends much less on the population index. In the displayed range of population indices in Figure 4 it varies between 2.2 and 2.7. In addition, the error bounds are much tighter due to the higher meteors counts available in the airborne data set.

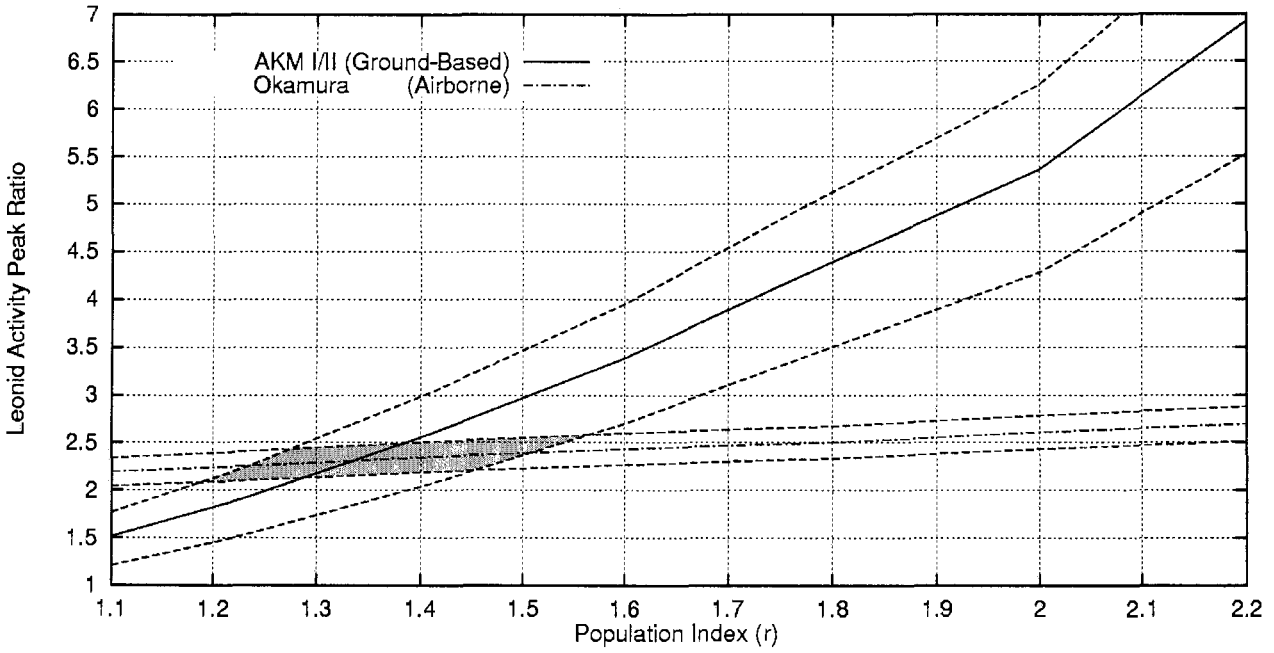

Figure 4 – Ratio of the normalized peak activity during the Asian and American Leonid storm as a function of the population index for the two ground-based and airborne cameras. Different observing geometries for both data sets results in two independent graphs (plotted with upper and lower error bounds) and an intersection area (shaded region) of values that are consistent with both data sets. Under the assumption that the population index was the same for both peaks, we find a most probable peak ratio of 2.3 at $r = 1.35$.

There is an area of intersection between the graphs for the ground-based cameras and for the airborne camera (shaded region in Figure 4). Population index and peak activity ratio pairs within that region are consistent with both data sets. We find that population indices between 1.2 and 1.55 and peak ratios between 2.1 and 2.6 are possible within the error bounds of our observations. The most probable solution is $r = 1.35$ and a peak ratio of 2.3. Whereas the peak ratio matches now perfectly the value found from visual observations, the population index is in strong disagreement.

9. Video based confirmation of population index

To confirm our result, we did a detailed analysis of the meteor brightness distribution for the two ground-based cameras. We manually estimated the peak brightness of all meteors that were automatically detected by the MetRec software. Reference stars between magnitudes +1 and +6 were used for brightness calibration, and even brighter meteors were estimated with reference to Jupiter's magnitude. The resulting plot of cumulative meteor counts (Figure 5) was somewhat surprising.

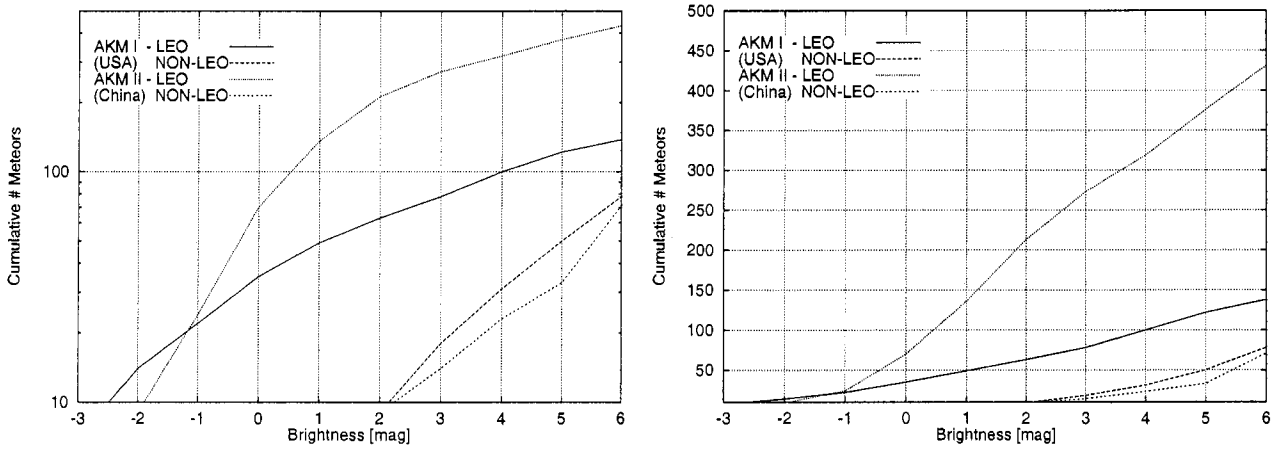

Figure 5 – Brightness distribution of Leonid and non-Leonid meteors for the two ground-based cameras. For the expected exponential increase in cumulative meteor numbers, the graphs need to be straight lines in a log-linear plot (left). That is approximately the case for non-Leonids, but not for the Leonids. They form a straight line in the linear-linear plot (right), which indicates that there was almost a constant number of meteors in each magnitude class fainter than −1 mag!

Normally we expect an exponential increase in cumulative meteor counts per magnitude class with the population index as the exponent. This would result in a straight line when cumulative meteor counts per magnitude class are plotted in a log-linear diagram (Figure 5, left). This is approximately true for the brightness distribution of all non-Leonid meteors, but certainly not for the Leonids. In fact, the Leonid distribution forms an almost a straight line in a linear-linear plot (Figure 5, right). In other words we observed approximately a *constant* number of Leonids per magnitude class in the brightness range between 0 and +6 mag! This result cannot be explained by lower detection probabilities for faint meteors, as meteors of +4 mag are so bright that they are easily picked up by the software, and the probability of detecting even a +5-mag meteor is still very high.

We repeated the meteor simulation with a change in the incident magnitude distribution such that it was represented by a constant meteor count in every magnitude class beginning at 0 mag with no meteors of negative magnitude. The result was that one obtains nearly the same detection efficiency ratios as found with exponential meteor counts whose population index was slightly above $r = 1.3$. Hence the measured meteor counts in each magnitude class provide an independent confirmation of a mean population index on the order of 1.3 to 1.4.

In summary, two methods to determine r give the same result. One is based on simple meteor counts of all three cameras (assuming that the population index was the same for both peaks), and the other on the Leonid brightness distribution found in the ground-based camera data. Note that even if there are approximately constant meteor counts per magnitude class, it would still make sense to work with an exponential distribution in the simulation for a specific small value for r. We want to apply the distribution to correct for different limiting meteor magnitudes. Thus, we need to know the increase in cumulative Leonid numbers for faint meteors near the camera limits which is indeed close to exponential (straight line for magnitude classes +3 to +6 in Figure 5, left).

10. Final simulation results with $r = 1.35$

We did a final meteor simulation run with a fixed population index of 1.35. The resulting time-dependent detection efficiencies for all cameras are presented in Figure 6 corrected for radiant altitude. Contrary to the initial simulation for $r = 2.1$, both ground-based cameras now have a flat response over time. This is because most of the Leonids are quite bright and losses due to lower limiting meteor magnitude caused by higher angular velocities have less impact. The airborne camera was on average almost one order of magnitude more efficient in detecting Leonids than the ground-based systems, which reflects quite well the absolute number of recorded Leonids on the ground versus onboard the airplane.

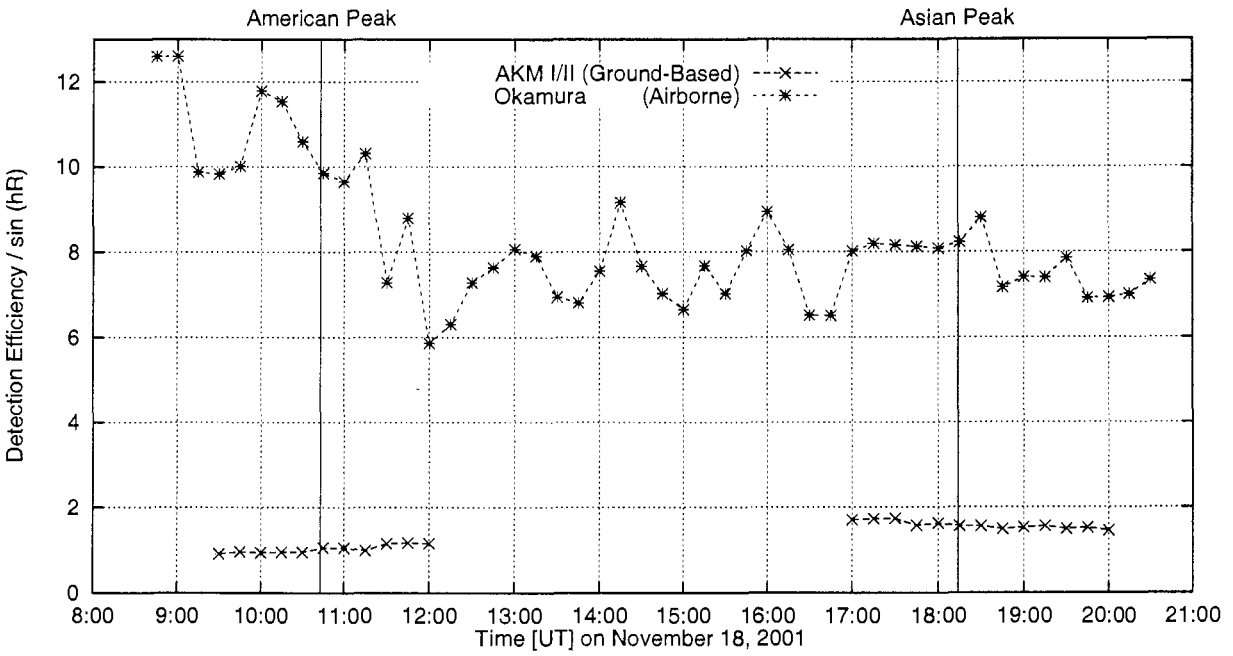

Figure 6 – Detection efficiencies for the three camera systems under changing radiant positions, limiting magnitudes, and pointing directions for a population index of $r = 1.35$. The influence of the variable radiant altitude has been removed to emphasize the contribution of the camera pointing direction.

11. Normalized activity profiles

Figures 7 and 8 show the activity profiles for both data sets similar to Figure 2 and 1, but now corrected for the detection efficiency with a population index of $r = 1.35$ (Figure 6). Due to large data scatter especially in the ground-based measurements it is difficult to give a quantitative description of the profiles and calculate the full-width half-maximum (FWHM) from the raw data. For this reason we tried to fit functions of different shapes to the activity profiles. We started with the airborne data set, because it contains a more continuous measurement record between the peaks.

At first, we tried to fit two Gaussians with a constant background component to the data, but we were not able to find a reasonable match. Then we replaced the Gaussians by two Lorentzian profiles as proposed by Jenniskens et al. (2000), and the fit with the minimum squared error matched the observed overall profile very well (Figure 7). The best match for the airborne data was achieved with a center time of 10^h39^m UT for the American and 18^h21^m UT for the Asian storm. It is no surprise that these times derived from smooth profiles differ slightly from the times of the narrow activity spikes determined earlier. The full width at half maximum is 108 min for the American and 120 min for the Asian storm. The normalized activity profiles consist of a constant background component of 0.63 Leonids/min and peak contributions by the two Lorentzians of 2.46 and 6.41 Leonids/min, respectively. Thus, we obtain the same peak ratio of 2.3 as in the earlier analysis. If we subtract the background component and look only at the widths and the peak values of the two Lorentzians, the FHWM reduces to 83 and 109 min, respectively, and we find a slightly larger peak ratio of 2.6 for the storm components.

We were not able to find a sensible fit for a third Lorentzian placed at the time of the early Asian peak (17^h39^m UT). The temporal width of the third profile was always one order of magnitude smaller than for the main Asian peak, which is highly improbable. Thus, if we believe in Lorentzian shaped profiles, linking this early peak to the passage of the 9-revolution trail is rather questionable. This leaves two other options:

(a) If the 9-rev and the 4-rev dust trails were encountered by the Earth in very short succession, we would not be able to separate their individual contributions in the observed Asian profile. All we have is the sum of both activity profiles. In this case, the observed peak activity is a lower bound for the sum of the peak activity of both trails, since only if they occurred at *exactly* at the same time would the trails add up to a maximum.

(b) If the 9-rev trail was much weaker than the 4-rev trail, it essentially would be lost in the observed Asian profile. In this case, the 9-rev trail could have been passed unnoticed at any time, and the observed Asian peak time and activity could be almost completely attributed to the younger 4-rev trail. The measured peak activity would be an upper bound for the 4-rev trail, since a minor contribution from the 9-rev trail would still be possible.

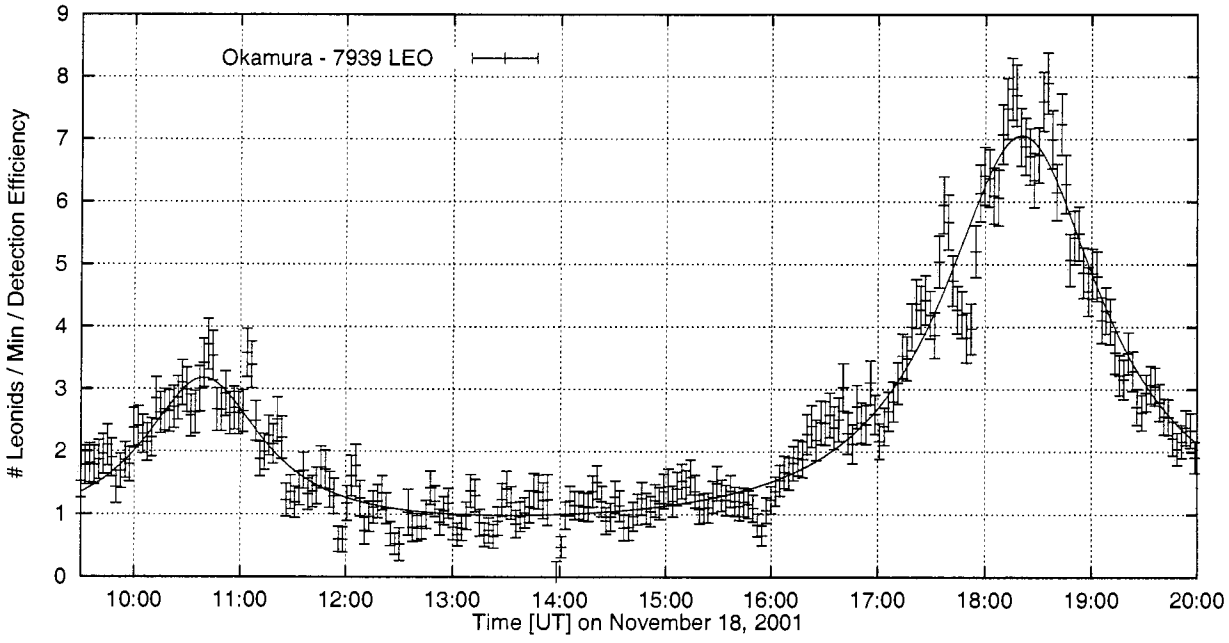

Figure 7 – Leonid activity curve for the Japanese airborne data. Leonid counts are corrected for the topocentric time of the stream encounter and the detection efficiency (see Figure 6). They are averaged in 5-min bins with 2.5 min shift, error bars are given for $\sqrt{n_{\mathrm{LEO}}}$. Two Lorentzian profiles together with a constant background component were fitted to the Leonid data.

For the ground-based data set, it was difficult to fit two Lorentzian profiles and the background component at the same time, as there were too many degrees of freedom. Thus, we took the background component from the airborne data scaled down by the peak ratios in the airborne and ground-based data. With the background fixed at the resulting 0.42 Leonids/min, the parameters of two Lorentzian profiles with the minimum squared error fit were determined (Figure 8). We found center times of 10^h42^m UT for the American and 18^h18^m UT for the Asian storm, which agree to within three minutes with the airborne data. The full width at half maximum including the background component matched well with the airborne data for the American storm (107 min), but for the Asian peak we found a significantly smaller value (98 min). The two Lorentzians have normalized peak values of 1.56 and 4.68 Leonids/min, respectively. That yields a peak ratio of 2.6 including the constant background. Profile widths and a peak ratio for the Lorentzians alone will not be given as they depend heavily on the background component, which could not be estimated from these data.

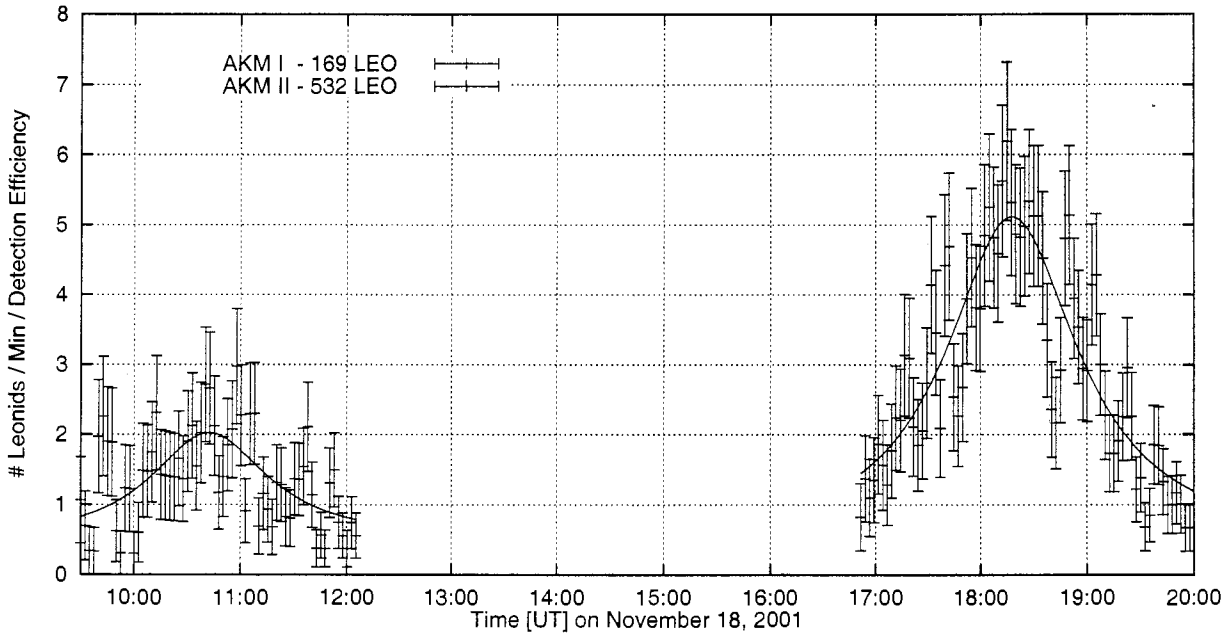

Figure 8 – Leonid activity curves for the two German cameras AKM I and II. Leonid counts are corrected for the topocentric time of the stream encounter and the detection efficiency (see Figure 6). They are averaged in 5-min bins with 2.5 min shift, error bars are given for $\sqrt{n_{\mathrm{LEO}}}$. Two Lorentzian profiles together with a constant background component were fitted to the Leonid data.

12. Evaluation of the Leonid storm predictions

Given the derived activity peak times and ratios we conclude that similar to the previous year the model of Lyytinen et al. (2001) was best at predicting the storms. Their peak time predictions for the main 7-rev and 4-rev trails were closer to the observed maxima than those of McNaught/Asher (2001) and Jenniskens (2001b).

Given the scenario (a) that both the 9-rev and the 4-rev trail occurred at almost identical times, the model of Lyytinen et al. was also best in predicting the passage time of the 9-rev trail, since they forecasted the smallest time difference between both trails. They have somewhat overestimated the peak ratio of the combined Asian relative to the American peak. We found a lower bound of 2.3 (or 2.6 when discarding the background component), and they predicted 3.8. Still the relative error is smaller than that of the flux ratio prediction of McNaught/Asher (12.5) and Jenniskens (1.1).

If the encounter follows scenario (b), where the Asian storm is almost completely attributed to the 4-rev trail, the prediction of Lyytinen et al. is still the winner. In this case, we find an

upper bound of 2.3 (or 2.6 when discarding the background component) for the ratio of the 4-rev and the 7-rev trail, which compares to a prediction of 2.5 by Lyytinen et al., 10.0 by McNaught/Asher, and 0.6 by Jenniskens. With respect to the strength of the 9-rev trail, all three predictions would be wrong in this scenario.

We conclude that taking into account the non-gravitational effects which distinguish the model of Lyytinen et al. (2001) from the one of McNaught and Asher (2001) gives a better description of the real meteoroid distribution and position in space. We cannot confirm the shift of dust trails suggested by Jenniskens (2001b) as neither the timing nor the nominal strength of the peaks in his prediction were closer than the other models. Even if one resorts to his extreme error limits our measured flux ratio falls outside his predictions.

13. Lessons learned

Observing on a commercial flight you are bound to the flight direction of the airplane. As a ground-based observer, however, you can optimize the data output by choosing an optimal observing direction. In 2001 there were no detailed instructions for the operators of the two AKM cameras during the Leonid storms. The observers were informally told to point the cameras at medium altitude and distance from the radiant. In the case of the American camera the instructions were not followed which turned out to be of great help in the analysis of the storms. Both cameras experienced different observing conditions, which complemented each other well. But what is the setup of choice for future video observations like the 2002 Leonid storms? How should the observers be instructed to get the best possible profile?

We propose to operate two similar or preferably identical unguided video cameras at each location (i.e. two pairs sited in Europe and North America during November 2002). One camera will be oriented such that at the time of the expected peak activity, it is pointed slightly below the radiant. As we have seen from the analyses presented above, the detection efficiency of a camera looking near the radiant is almost independent of the population index of the shower (additional simulations have shown that the point of weakest dependency is in fact located somewhat above the radiant). Hence, this camera can be used to determine the absolute level of flux even if r is unknown. The activity profile, on the other hand, will be less accurate because for larger r-values the detection efficiency changes dramatically over time as the radiant approaches and leaves the field of view. We propose a FOV *slightly* below the radiant to have the camera pointed at a lower elevation and monitoring a larger atmospheric volume towards the horizon. For major showers with lower population indices, this results in a larger number of meteor recorded and improved statistics.

The second camera of a given site would be pointed at the same low elevation angle as the first, but at a large distance from the radiant (preferably 60° or more). In that direction, the detection efficiency is very sensitive to the population index as shown in the previous sections, but it changes only marginally with time as the radiant distance remains large. Thus, the absolute flux level is difficult to determine with this camera, but it provides an accurate activity profile over time. The scaling of the profile can be taken from the first camera. The advantage of pointing the two cameras at the same elevation is to observe the same atmospheric volume under the same conditions (e.g. atmospheric extinction). This reduces systematic errors, as the simulation can only approximately account for the extinction losses, which may have some variance between the actual site and the loss model implemented in software. A combination of counts from both cameras finally yields the population index independent of meteor brightness measurements as demonstrated in section 9.

In the presence of a bright moon, some variation from this general setup may be necessary (e.g. one may try to have both cameras looking at about the same angular distance from the moon), but still one camera should be pointed close to and the other far away from the radiant at identical low elevation angles.

14. Conclusions

We analyzed two independent video data sets from the 2001 Leonid storms. One was obtained using two identical ground-based cameras operated in the USA and China, the second one came from an airborne camera that flew over the Pacific Ocean and recorded both peaks. We derived detailed activity profiles that were corrected for the radiant altitude and the topocentric time of the stream encounter. Initial meteor simulations to account for the different observing geometry (observing direction, angular distance to the radiant, true meteor distance, extinction) resulted in large discrepancies between the data sets. After we ruled out a number of possible error sources we found that the assumed population index of $r = 2.1$ was not consistent with our data. However, both the ground-based and the airborne data match each other if we assume an identical population index for both peaks of $r = 1.35$. A detailed analysis of the meteor brightness distribution in the ground-based video data confirmed virtually the same population index for faint meteors.

The low population index of $r = 1.35$ is in strong disagreement with the value obtained from visual observations (Arlt et al. 2001). We do not believe that the visual results are in error, but that there is some systematic shift in meteor brightnesses in the video record which we do not yet understand. It might be linked to a different spectral or temporal response of intensified video cameras compared to the human eye, but the solution is not straight forward because reference stars used for the magnitude calibration would experience a similar effect.

For the American Leonid storm caused by the 7-rev dust trail, we find two activity peaks at 10^h43^m and 11^h02^m UT which confirms the peaks that were found at almost identical times in the visual data (Arlt et al. 2001). A Lorentzian fit to the profile yields a center time of 10^h40^m UT and a full width at half maximum of 108 minutes. Also the peak time of the Asian storm at 18^h14^m caused by the 4-rev trail agrees to within minutes with the visual results. Here the Lorentzian fit is centered at 18^h20^m UT. The average full width at half maximum of both data sets is 109 min, but the ground-based and the airborne profile do not agree well here. The airborne data show an early spike of activity at 17^h39^m UT, and at the same time there is also a local peak in the ground-based profile. An association with the 9-rev trail is still questionable, because of the small width of the peak. Overall we find a peak activity ratio of 1:2.3 between the American and the Asian storm. The true ratio of the individual storm components is somewhat higher, as this figure also includes a background component.

Both the times of the main peaks and their relative peak ratio were best predicted by the model of Lyytinen, Nissinen and van Flandern (2001). The non-gravitational effects, which make their prediction different from the McNaught and Asher (2001) model, seem to give a better description of the real meteoroid distribution. The shift of dust trails suggested by Jenniskens (2001b) is not confirmed by our data, as neither the timing nor relative strength of the peaks were better predicting by his theory.

For future observing campaigns, we propose to operate two identical unguided cameras at each observing site. One of them should be pointed slightly below the radiant at the expected peak time, and the other one at the same elevation angle but at large distance from the radiant, which will optimize the data output.

15. Addendum

At the time of submittal of this paper for publication another independent data set became available to one of the authors (P.G.) This included some ground based and airborne intensified video imagery from the 2001 Leonid Multi-Instrument Aircraft Campaign (Leonid MAC). We would like to thank Peter Jenniskens for making this data set available for our analysis. The Leonid MAC mission instrumentation had been setup in several locations around the world which included a standard design 50-mm $f/1.4$ lens coupled to an AEG MCP generation II image intensifier whose output was recorded on a Sony Hi-8 camcorder (Gural & Jenniskens 2000). Two ground-based cameras were choosen for the analysis. One of them recorded the American peak

at a site on Mount Lemmon, Arizona, the other observed the Asian peak a few kilometers outside of Alice Springs, Australia. The tapes span the rising and falling activity profiles of both storms. However, in a first analysis Peter Gural concentrated on the peak flux period and reviewed only a ten minute segment of time centered around each of the activity maxima. Several repeated inspections of the tapes were made to insure maximizing meteor detection statistics. For the American peak, 45 Leonids and 2 non-Leonids were detected between 10^h40^m–10^h50^m UT. The raw counts for the Asian peak between 18^h10^m and 18^h20^m were 21 Leonids and 5 non-Leonids. The meteors were tabulated and stream associations verified using both visual monitoring and the MeteorScan automated detection software. A summary of the camera orientations and observing conditions are listed in Table 3.

Table 3 – Leonid MAC ground based camera specifications for the near-radiant pointing Mt. Lemmon, USA, imager and the southerly pointed Alice Springs, Australia, imager.

Camera	Mt. Lemmon (America)	Alice Springs (Australia)
Location	32°.25 N / 111°.03 W	23°.7 S / 133°.87 E
Pointing center [azimuth/altitude]	122° / 53°.5	171° / 37°.1
Diameter of field of view	41° circ. / 31° cutoff	35° circ. / 26°.3 cutoff
Spatial resolution [arcmin/pixel]	3.9	3.3
Integration time [s]	0.0167	0.0167
Stellar limiting magnitude [mag]	+7.4	+7.4
Height [km]	2.8	0.0

Detection efficiencies as a function of population index were obtained for the camera systems and the same analysis applied as described earlier for the flux number versus population index. After correction for the detection efficiency another curve of the Leonid peak ratio vs. population index similar to Figure 4 was obtained. The resultant ratio varied from a high of 5.62 at $r = 2.2$ through a mid-range value of 3.16 at $r = 1.6$, to a low of 1.80 at $r = 1.23$ with the curve falling between the two previous curves of Figure 4. What is astounding is that the third independent data set curve crosses through the same intersection point of the other two sets at a population index of $r = 1.35$ and flux ratio of 2.3! This further confirms the r-value and the peak activity ratio of the two Leonid storms as determined in this paper's analysis.

References

Arlt R., Bellot Rubio L., Brown P., Gyssens M., "Bulletin 15 of the International Leonid Watch: First Global Analysis of the 1999 Leonid Storm", *WGN* 27:6, 1999, pp. 286–295.

Arlt R., Gyssens M., "Bulletin 16 of the International Leonid Watch: Results of the 2000 Leonid Meteor Shower", *WGN* 28:6, 2000, pp. 195–208.

Arlt R., Kac J., Krumov V., Buchmann A., Verbert J., "Bulletin 17 of the International Leonid Watch: First Global Analysis of the 2001 Leonid Storms", *WGN* 29:6, 2001, pp. 187–194.

Asher D.J., "The Leonid Meteor Storms of 1833 and 1966", *MNRAS* 307, 1999, pp. 919–924.

Bevington P., "Data Reduction and Error Analysis for the Physical Sciences", McGraw-Hill, New York, 1969.

Brown P., Cooke B., "Model predictions for the 2001 Leonids and Implications for Earth-orbiting Satellites", *Mon. Not. R. Astron. Soc.* 326, 2001, pp. L19–L22.

Gural P., Jenniskens P., "Leonid Storm Flux Analysis from One Leonid MAC Video AL50R", *Earth, Moon and Planets* 82–83, 2000, pp. 221–247.

Gural P., "Meteor Observation Simulation Tool", submitted to *Proc. of the International Meteor Conference 2001,* Cerkno, Slovenia, 2001.

Hawkes R., *personal communications*, 1998.

Jenniskens P., Crawford C., Butow S.J., Nugent D., Koop M., Holman D., Houston J., Jobse K., Kronk G., Beatty K., "Lorentz Shaped Comet Dust Trail Cross Section from new Hybrid Visual and Video Meteor Counting Technique - Implications for Future Leonid Storm Encounters", in: P. Jenniskens, F. Rietsmeijer, N. Brosch, M. Fonda (eds.), *Leonid Storm Research*, Kluwer Academic Publishers, Dordrecht, 2000, pp. 191–208.

Jenniskens P., oral presentation at *Meteoroids 2001 Conference*, Kiruna, Sweden.

Jenniskens P., "Model of a One-Revolution Comet Dust Trail from Leonid Outburst Observations", *WGN* 29:5, 2001, pp, 165–175.

Kondrat'eva E.D., Reznikov E.A., "Coment Tempel-Tuttle and the Leonid Meteor Swarm", *Sol. Syst. Res.* 19, 1985, pp. 96–101.

Koschny D., Zender J., "Comparing Meteor Number Fluxes from Ground-based and Airplane-based Video Observations", in: P. Jenniskens, F. Rietsmeijer, N. Brosch, M. Fonda (eds.), *Leonid Storm Research,* Kluwer Academic Publishers, Dordrecht, 2000, pp. 209–220.

Lyytinen E., van Flandern T., "Leonid Predictions for the Years 1999–2007 with the Satellite Model of Comets", *Meta Research Bulletin* 8, 1999, pp. 33–40.

Lyytinen E., Nissinen M., van Flandern T., "Improved 2001 Leonid Storm Predictions from a Refined Model", *WGN* 29:4, 2001, pp. 110–118.

McNaught R.H., Asher D.J., "Leonid Dust Trails and Meteor Storms", *WGN* 27:2, 1999, pp. 85–102.

McNaught R.H., Asher D.J., "The 2001 Leonids and Dust Trail Radiants", *WGN* 29:5, 2001, pp. 156–164.

Molau S., "The AKM Video Meteor Network", in: B. Warmbein (ed.), *Proc. Meteoroids 2001 Conference,* Kiruna, Sweden, 2001, pp. 315–318.

Authors' addresses:

Sirko Molau, Weidenweg 1, D-52074 Aachen, Germany,
e-mail `sirko@molau.de`,

Peter S. Gural, 351 Samantha Dr., Sterling, VA 20164-5539, U.S.A,
e-mail `peter.s.gural@saic.com`,

Osamu Okamura, 5-11-4 Ibukidaihigashi-mati, Nishi-ku, Kobe, Japan,
e-mail `kobe.cpa.okamura@nifty.com`.

Ongoing Meteor Work

Annual Activity of the Alpha Aurigid Meteor Shower as Observed in 1988–2000

Audrius Dubietis and Rainer Arlt

The annual activity of the α-Aurigid meteor shower is analyzed using the records of the Visual Meteor Database. Apart from 1994 when enhanced activity of the shower was reported, the α-Aurigids produce a fairly stable maximum with average ZHR = 7 ± 1 at $\lambda_\odot = 158\overset{\circ}{.}6 \pm 0\overset{\circ}{.}1$. An average population index $r = 2.6 \pm 0.1$ was derived and found to possess a slight minimum around the time of maximum activity.

1. Introduction

The history of the α-Aurigid meteor shower is short but lively. It is best known for three unexpected outbursts in 1935, 1986, and 1994. The shower was probably discovered during the outburst in 1935 by German and Czechoslovak observers [1] reporting activity of up to 30 meteors per hour. The next two short-lived (within one hour) peaks have been observed in 1986 [2] and 1994 [3]. Although the observational data of two recent outbursts could be found in the Visual Meteor Database of *IMO* (*VMDB*), the ZHR profiles for them could be hardly regained because the original data is given in one-hour intervals or so. The 1986 outburst with ZHR = 27 ± 6 at $\lambda_\odot = 158\overset{\circ}{.}53$ is based on a single observation by Tepliczky from Hungary [2]. The 1994 outburst had a maximum ZHR of 30 ± 9 at $\lambda_\odot = 158\overset{\circ}{.}72$ and was witnessed by Zay and Lunsford in USA [3]. Taking into account that radio observations have detected the strong peak earlier [4], a potential activity in ZHR terms of a few hundreds was then deduced [5]. Ancient records of α-Aurigid observations are hard to trace. Several notes about meteors in the activity period of the α-Aurigid are found in the chronicles of the Beijing Observatory [6], especially for the end of the 19th century. But these records give notes like "meteors fell like rain" for dates all around the year, and there is no conclusive link to the α-Aurigids.

The α-Aurigid meteoroid stream has a well established parent body, the long period Comet C/1911 N1 Kiess. However, the observed outbursts are not associated with the perihelion passage of the comet which has a revolution period of the order of 2000 yr, but rather with short-periodic perturbances which may be expected from the giant planets—Jupiter and Saturn [5].

To date, the level of α-Aurigid annual activity is still ill defined and has been monitored just in recent decades. Some attempts based on relatively small numbers of meteors have brought to contradictory results: the maximum ZHR varies from 3 to 13 with the maximum date being uncertain in the solar longitude range within $157\overset{\circ}{.}5$ and $158\overset{\circ}{.}7$ (see Table 1).

Table 1 – Annual activity of the α-Aurigid meteor shower. B denotes the slope of double exponential fit, and r is the population index.

Maximum date	ZHR	B	r	Reference	Remarks
157.5 ± 0.5	9 ± 3	0.19 ± 0.04	2.7	[7]	1981–1991
158.0 ± 0.5	3.0 ± 1.0	0.50 ± 0.20	3.0	[5]	1992–1995
158.6	7.2 ± 2.1		2.5	[8]	1988–1995
158.7	13 ± 3		2.8	[8]	1997

The aim of this analysis is to obtain more reliable annual activity picture of the α-Aurigid meteor shower. Currently, the *VMDB* provides almost 3000 α-Aurigids, thus being a quite comprehensive data set for such an analysis.

2. Observations

Since the α-Aurigids are primarily a northern-hemisphere shower, only the observations from northern latitudes were included in the analysis. In total, 2931 observing intervals within the solar longitude range of 150° to 166° reporting 2813 α-Aurigids were found in the *VMDB*. The magnitude distributions are available starting with 1988; those include 2645 shower meteors. Seven more or less reliable individual ZHR profiles were constructed, whereas observational data from less successful years containing just raw counts around the shower maximum were used for the general activity profile. Table 2 summarizes the α-Aurigid data for the individual years. In addition, the uncovered gaps near the maximum larger than 0°.2 in solar longitude are listed.

Table 2 – The α-Aurigids in the *VMDB* in the period of $\lambda_\odot = 150°$ to 166° (observations from the southern hemisphere are omitted).

Year	Rate data		Magnitude data		Remarks
	Periods	N_{AUR}	Distributions	N_{AUR}	
1986	69	48	–	–	outbust
1987	47	71	–	–	poorly observed
1988	58	10	4	9	poorly observed
1989	125	192	35	175	gaps for $\lambda_\odot = 158°.04$–$158°.55$, $158°.81$–$159°.01$
1990	160	330	61	328	no observations after $\lambda_\odot = 158°$
1991	62	47	14	49	poorly observed
1992	105	131	30	146	uncovered gap $\lambda_\odot = 158°.04$–$158°.83$
1993	81	38	11	40	poorly observed
1994	102	101	19	96	outbust
1995	133	186	46	184	uncovered gap $\lambda_\odot = 158°.67$–$159°.02$
1996	96	41	15	41	poorly observed
1997	383	402	104	395	uncovered gap $\lambda_\odot = 158°.17$–$158°.50$
1998	223	242	45	227	
1999	334	261	54	254	uncovered gap $\lambda_\odot = 158°.26$–$158°.50$
2000	953	723	170	699	uncovered gap $\lambda_\odot = 158°.44$–$158°.64$
Total	2931	2813	607	2645	

3. Population index

The population index has been calculated using the same considerations as described in our previous paper [11]. The datasets of all the years separately were too small to derive reliable graphs of the population index. Only the combined data were found to be useful for the computation of the entire r-profile. The complete magnitude dataset gives an average $r = 2.61 \pm 0.05$, and a similar value of $r = 2.59 \pm 0.06$ was obtained from a reduced dataset ($\mathrm{lm} \geq +5.80$) consisting of 2270 meteors in 487 magnitude distributions. The population index profiles have been constructed for these two cases as shown in Figure 1. There is no strong variation of the population index with the solar longitude, however, lower r-values match the activity maximum and a time around $\lambda_\odot = 155$ where a shoulder in the activity curve is present (cf. Figure 6 for both features).

4. Activity profiles

A standard procedure has been used for the activity profile calculation. Averages of the ZHR for a given time period were calculated considering small-number statistics [12]:

$$\overline{\mathrm{ZHR}} = \left(1 + \sum_i n_i\right) \Big/ \sum_i \frac{T_{\mathrm{eff},i}}{C_i} ,$$

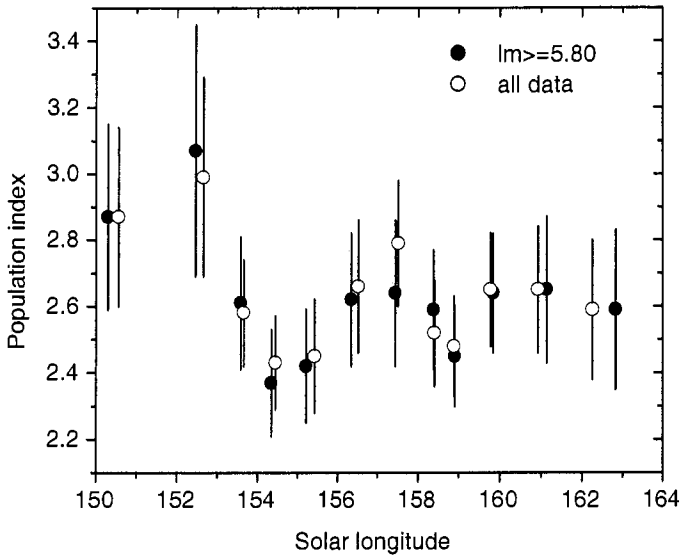

Figure 1 – Population index profile of the α-Aurigids.

where n_i is the individual number of shower meteors observed during a time period $T_{\mathrm{eff},i}$, and C_i is the total correction for the limiting magnitude lm, field obstruction factor F, and the radiant elevation h_{R}:

$$C_i = r^{(6.5-\mathrm{lm})}\, F \,/ \sin h_{\mathrm{R}}.$$

Only the observations that fulfill the condition $C_i < 8$ were used in the ZHR calculation. For the α-Aurigids, the above condition is more convenient than $C_i < 5$, since a more strict data selection reduces the available dataset by additional about 20%. A constant $r = 2.6$ was assumed.

A few remarks on the data treatment should be given here. There is a clear distinction in the *VMDB* whether the shower produced no meteors, or it has not been observed at all. Nevertheless, care should be taken here. On several occasions, observers introduce a weak meteor shower in their reports only after they had seen a meteor from that radiant. While they have certainly included the α-Aurigids near maximum, even if they saw no meteors from that radiant (since they were "going out for them"), they might have omitted the information "no meteor seen" from the report several days before or after the expected peak. Since these negative detections may be missing, the ZHRs at the far ends of the activity period may be overestimated. In particular, this could be a reason for a constant background with ZHR = 2 to 3 in the activity profile (for instance, the profile given in [8]). We would like to stress again the importance of including zero-detections in meteor reports.

In this analysis, all the observational data in the solar longitude interval from 150° to 166° was used, and where the α-Aurigids were not explicitely given, we assigned "0 observed shower meteors" to the observations. At the far ends of the activity profile, this will certainly result in lower limits of the activity, while the assumption will have negligible effect near the maximum of the shower when AUR is given in almost every report.

For the individual year ZHR estimates 1° bins were applied across the whole activity period. The relatively large bin size was imposed by the small number of observations. A fit function [7]

$$\mathrm{ZHR} = \mathrm{ZHR}_{\max} \exp\left(B|\lambda_\odot - \lambda_\odot^{(\max)}|\right)$$

was used to derive the shower parameters. $\mathrm{ZHR}_{\max}$ is the maximum activity level, $\lambda_\odot^{(\max)}$ is the time of maximum (all solar longitudes refer to J2000.0). B is the inverse width of the profile, and the full width of half-maximum is then

$$\mathrm{FWHM} = \log 2 \times 2/B.$$

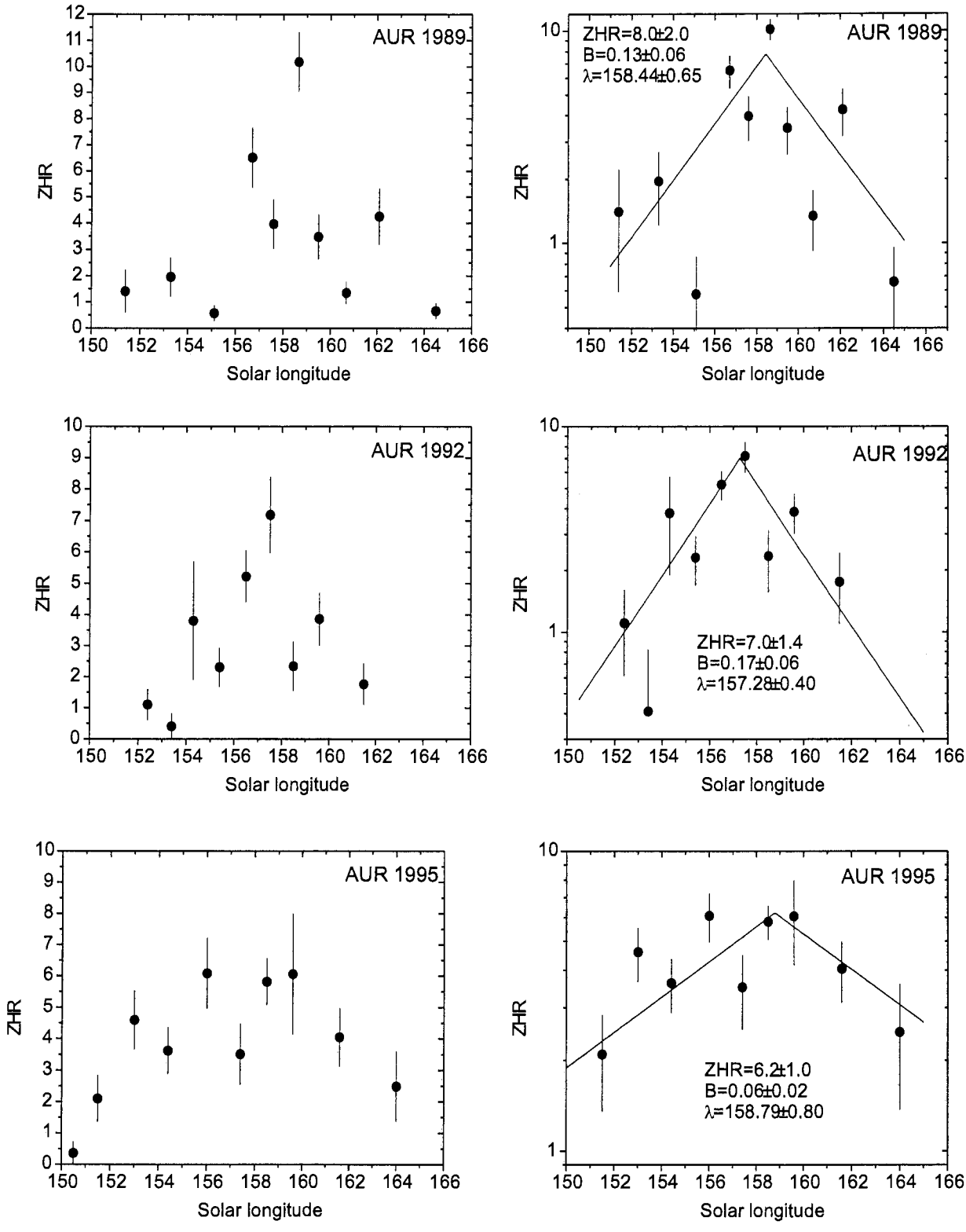

Figure 2 – Individual activity profiles of 1989, 1992, and 1995. Data points in right graphs are plotted in the logarithmic scale and two-side exponential fit is shown by a solid line.)

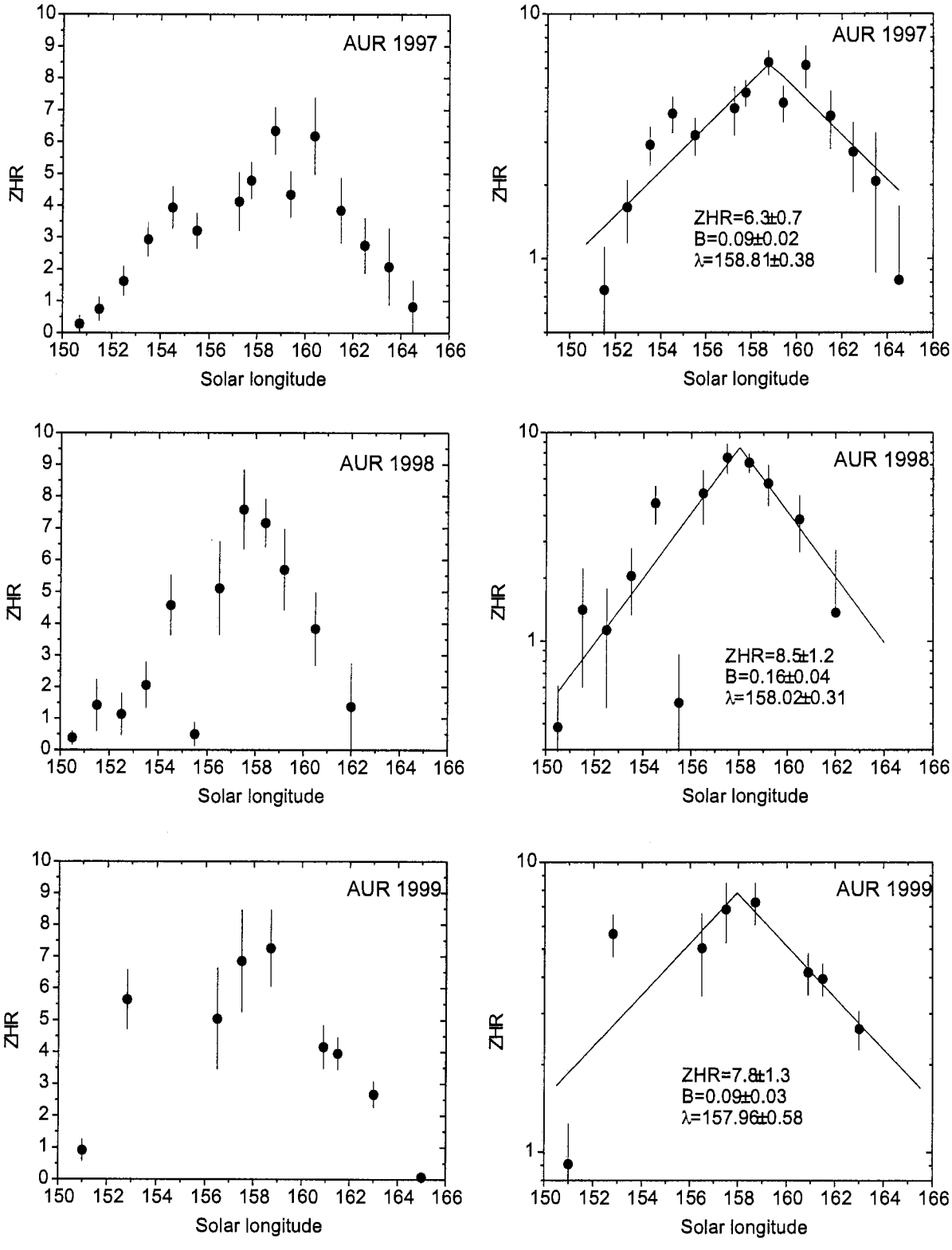

Figure 3 – Individual activity profiles of 1997–1999. Data representation is the same as in Figure 2.

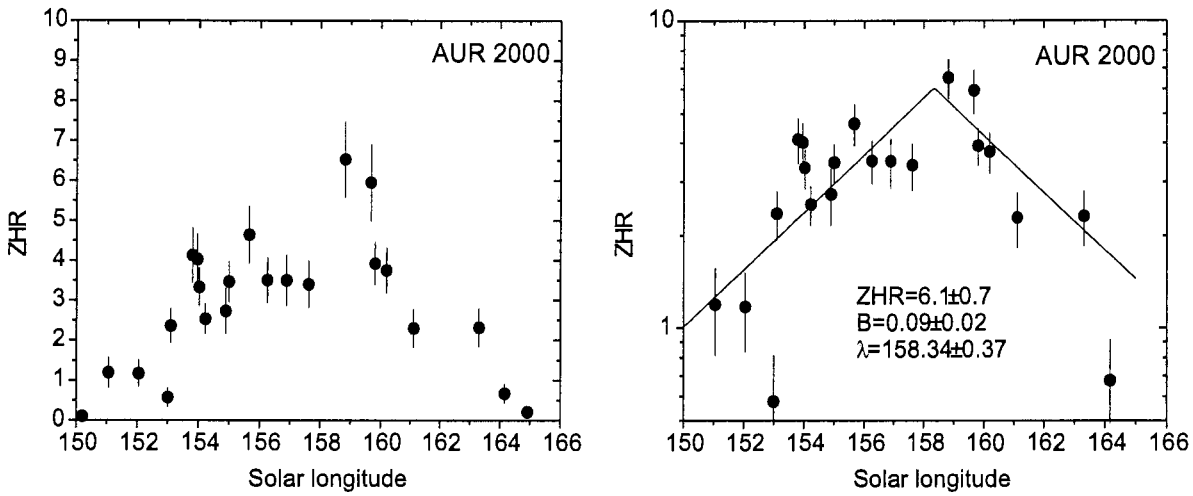

Figure 4 – Individual activity profile of 2000. Data representation is the same as in Figures 2 and 3.

Observations of 1990 are not presented in the graphs as only the ascending branch of the activity curve was observed with very few reports around the shower maximum. The same applies to the observations of 1994; only the descending branch was recorded. Moreover, the 1994 outburst data is given in 1-hour intervals, and simple averaging within 1° bins yields just normal activity of ZHR = 8.0 ± 1.1 at $\lambda_\odot = 158.^\circ6$. Figures 2, 3, and 4 show the individual ZHR profiles and the fit functions in logarithmic scale. The summary for the shower parameters is given in Table 3.

No strong variation of shower activity from year to year has been found. $\mathrm{ZHR_{max}}$ typically exceeds rates of 6 to 8, with maximum times between $\lambda_\odot = 158.^\circ5$ and $158.^\circ8$. Some earlier maxima at $\lambda_\odot = 157.^\circ5$ (in 1992 and 1998) might have simply resulted from a lack of data and other observational features. The early maximum in 1992 is definitely a result of missing observations between $\lambda_\odot = 158.^\circ42$ and $158.^\circ83$ (see Table 2). For the 1998 maximum, we have two competing values: ZHR = 7.6 ± 1.3 at $\lambda_\odot = 157.^\circ5$ and ZHR = 7.2 ± 0.8 at $\lambda_\odot = 158.^\circ4$. The latter ZHR value is derived from a larger number of observations, so we consider it a true maximum in Table 3. On the other hand, the shower parameters derived from the fit functions exhibit a continuous scatter in maximum dates. No correlation between the time of maximum and the strength of the highest ZHR is found. Also the B slopes vary by a factor of almost three. Anyway, the most typical B of ~ 0.1 could be deduced. It corresponds to a FWHM shower width of $\sim 6°$.

The 2000 activity profile suggests a rather strong shoulder of ZHR = 3–4 at solar longitudes from $\lambda_\odot = 154°$ to 158°. A similar feature is also clearly present in the 1997 activity profile. More observational data should clarify whether this feature is permanent, temporary, or just associated with observational specifics. The significance is—given the minimum in r at the same time which even tends to reduce rates—quite high, and we consider this structure a topic of further studies.

Figure 5 depicts the combined activity profile obtained from 2833 observations in 1988–2000 (1995 of them fulfill the condition $C_i \leq 8$). Each data point represents an average of 90 observing periods that are grouped within $0.^\circ5$–1° bins. The asymmetry in the combined profile drags the fitted two-side exponent to smaller solar longitudes than the maximum ZHR average suggests. The difference of the peak of the fit and the moment of highest observed ZHR is $0.^\circ5$. Since the fitting could hide a physical asymmetry, we prefer to give the time of highest ZHR as the peak time of the α-Aurigids.

An important criterion of data selection is the radiant altitude h_R. The α-Aurigid radiant reaches a reasonable elevation ($h_\mathrm{R} > 30°$) just after local midnight, so the evening observations

might cause some systematic errors due to the effects related to the low radiant altitude and a possible zenithal exponent $\gamma \neq 1$ (usually $\gamma = 1$ in the expression $\cos^{\gamma} h_{\mathrm{R}}$ is assumed) [13, 14]. Surprisingly, the additional limitation of $h_{\mathrm{R}} > 20°$, which is often applied in similar cases, has not altered the ZHR profile much and preserved the same features (see open circles in Figure 6), while the dataset has been notably reduced—from 1995 to 1383 observing periods. Only at the time of maximum activity, the ZHR level is significantly reduced as low-radiant periods are omitted. Neglecting the highest filled circle in Figure 6, we note a fairly linear decay of the shower at both ends, except for the plateau between 154° and 156°.

Table 3 – Observational and fitting data summary for the α-Aurigid meteor shower.

Year	Observational data		Fitting data		
	$\lambda_{\odot}^{(\max)}$ (J2000)	$\mathrm{ZHR}_{\max}$	$\lambda_{\odot}^{(\max)}$ (J2000)	$\mathrm{ZHR}_{\max}$	B
1989	158.65	10.2 ± 1.1	158.44 ± 0.65	8.0 ± 2.0	0.13 ± 0.06
1992	157.5	7.2 ± 1.2	157.28 ± 0.40	7.0 ± 1.4	0.17 ± 0.06
1995	158.5	5.8 ± 0.8	158.79 ± 0.80	6.5 ± 1.0	0.06 ± 0.02
1997	158.75	6.4 ± 0.7	158.81 ± 0.38	6.3 ± 0.7	0.09 ± 0.02
1998	158.4	7.2 ± 0.8	158.02 ± 0.31	8.5 ± 1.2	0.16 ± 0.04
1999	158.7	7.3 ± 1.2	157.96 ± 0.58	7.8 ± 1.3	0.09 ± 0.03
2000	158.8	6.5 ± 1.0	158.34 ± 0.37	6.1 ± 0.7	0.09 ± 0.02
Overall	158.62	7.2 ± 0.4	158.13 ± 0.20	6.5 ± 0.4	0.10 ± 0.01

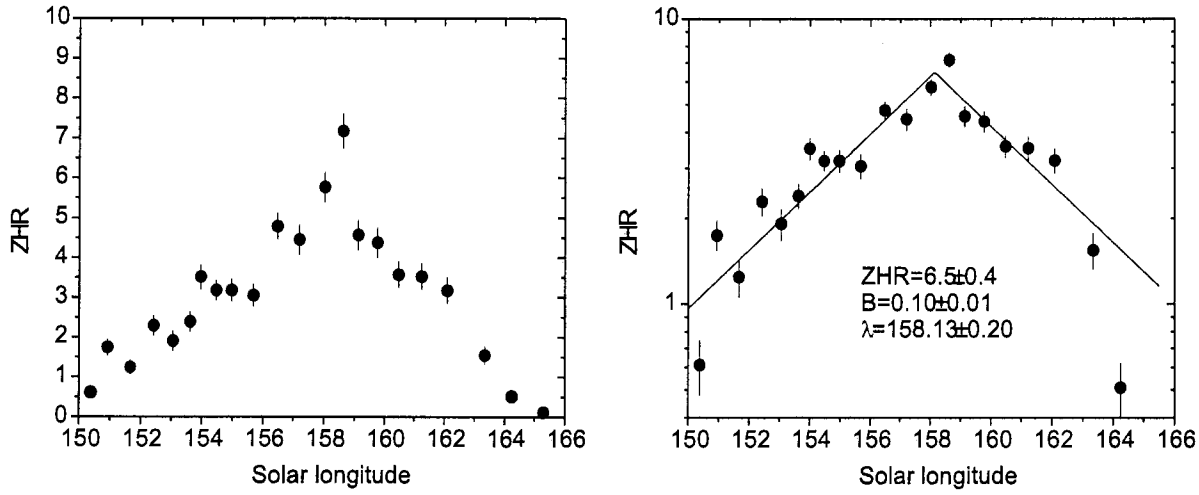

Figure 5 – Combined activity profile of 1988–2000 observations, using a constant population index of $r = 2.6$. The left graph shows two-side exponential fit.

5. The 1994 outburst

The observational data of 1994 were too scarce to build an entire activity profile. However, this year was exceptional for the unexpected outburst [3]. Although it was much better documented than the previous two, there are still large unfilled gaps in the observational data. The outburst data contains 76 shower meteors in 34 observing periods in a solar longitude range $\lambda_{\odot} = 157\overset{\circ}{.}28$ to $159\overset{\circ}{.}83$ provided by 11 observers.

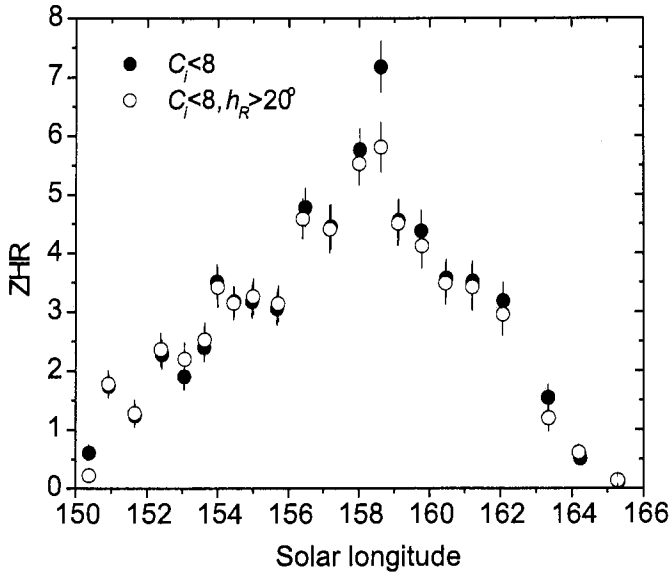

Figure 6 – Combined activity profiles calculated using different data selection criteria. The filled circles are the same as in Figure 5.

Figure 7 shows a *qualitative* picture of the outburst. The observations available are too few, so the final result is strongly dependent on the number of observing periods averaged and the choice of the bin size. Each data point in the background is an average of 3–6 observing periods, whereas the two outburst data points were obtained from two observing periods each. The data suggest ZHR = 45±10 at $\lambda_\odot = 158.^\circ74$. The population index was assumed to be $r = 2.15 \pm 0.18$, as derived from the 1994 magnitude distribution, containing 96 meteors, with vast majority of them (76) seen between $\lambda_\odot = 157°$ and $\lambda_\odot = 160°$. The solid line is the annual activity curve obtained from the 1988–2000 fit (the same as in Figure 5). The peak is roughly 3 hours after the average peak time as derived from the graph in Figure 5. This is not much given the large scatter of maximum times for individual years. of the ann

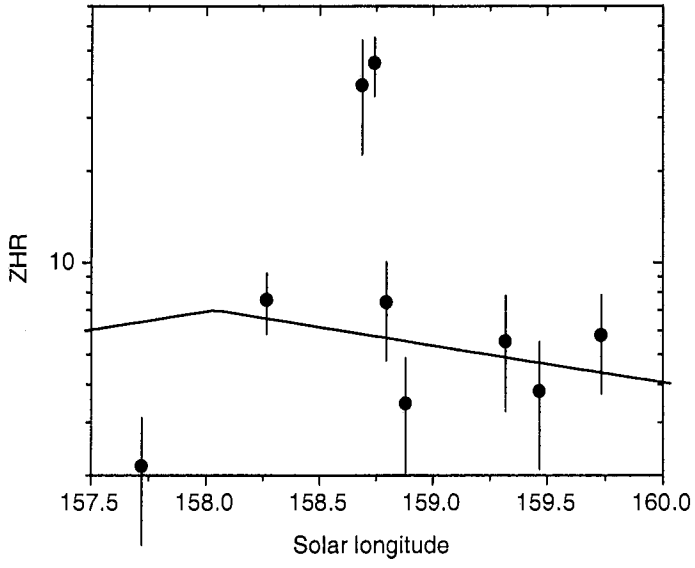

Figure 7 – Qualitative picture of the 1994 outburst. The solid line denotes the fit for the annual activity profile of 1988–2000.

6. Conclusions

More than one decade (1988–2000) of observational data from the *VMDB* was used to analyze the annual activity of the α-Aurigid meteor shower. It was found that the level of the shower's annual activity remains almost constant through the years with typical ZHR = 7 at $\lambda_\odot = 158\overset{\circ}{.}6$. The exact maximum time seems to fit in the interval from $\lambda_\odot = 158\overset{\circ}{.}5$ to $158\overset{\circ}{.}8$. The values obtained are in good agreement with those given in the *IMO* Working List of meteor showers.

In addition, a graph of the entire activity profile was obtained. It suggests the existence of a long shoulder within the period from $\lambda_\odot = 154°$ to 158° with ZHR = 3*to*5. The fact that notable activity is somewhat more extended in time before the maximum than after it, may be partly due to interference with late Perseids. The distinction of the two showers is difficult for observing fields in southern direction. Interference with δ-Aurigids which peak near September 8 on $\lambda_\odot = 166°$ is not obvious in the activity graph in Figure 5 although they are close in position, too. Both facts together indicate that the skew of the profile is significant. In general, the activity period given in the *IMO* Working List is found to be adequate for the α-Aurigids; it might be extended by a few days to September 7 or 8 ($\lambda_\odot \approx 165°$).

The r-profile reveals that the shower maximum coincides with the minimum of the population index, or lies slightly before that minimum. The significance of the population index variations is poor though, and an even deeper minimum occurred near $\lambda_\odot = 155°$ which coincides with the strongest part of the shoulder in Figure 5. We suppose that this is a distinct feature in the α-Aurigid meteoroid stream.

The maximum ZHR of about 7 can be converted—together with the population index of $r = 2.6$—into a spatial number density of particles in the meteoroid stream. We obtain a density of $\varrho_{6.5} = 17 \pm 4$ particles per 10^9 km^3. This is a very small number; the fact that we see a noticable meteor shower only results from the high relative velocity of 66 km/s with which we pass the meteoroid stream. Less than 1 particle per 10^9 km^3 exceeding a mass of 1 mg can be found in the α-Aurigid stream. The Perseids reach typically about 15 particles with masses larger than 1 mg at their maximum. A slow meteor shower like the Geminids (35 km/s) contain 200 of such particles in 10^9 km^3. Meteoroid streams with high velocities are thus much easier to detect than slow meteoroid streams.

The physical properties of the α-Aurigid stream and the origin of the outbursts make it comparable to the Lyrid meteoroid stream. Moreover, the observational characteristics of the shower (character of the annual activity profile with extended shoulder before the maximum and the population index profile) could be an additional strong argument in favor of this.

References

[1] C. Hoffmeister, "Unexpected meteor shower", *Astr. Nachr.* 258 (1936), pp. 27–30.

[2] I. Tepliczky, "The maximum of the Aurigids in 1986", *WGN* 15 (1987), pp. 28–29.

[3] G. Zay, R. Lunsford, "On a possible outburst of the 1994 alpha-Aurigids", *WGN* 22 (1994), pp. 224–226.

[4] P. Jenniskens, I. Yrjölä, P. Sears, W. Kuneth, T. Rice, "The global meteor-scatter network", *WGN* 25 (1997), pp. 141–144.

[5] P. Jenniskens, "Meteor stream activity IV. Meteor outbursts and the reflex motion of the Sun", *Astron. Astrophys.* 317 (1997), pp. 953–961.

[6] I. Hasegawa, "Historical Records of Meteor Showers", In: J. Štohl, I.P. Williams (eds.): *Meteoroids and their parent bodies*, 1993, pp. 209–223.

[7] P. Jenniskens, "Meteor stream activity I. The annual streams", *Astron. Astrophys.* 287 (1994), pp. 990–1013.

[8] J. Rendtel, R. Arlt, A. McBeath, "Handbook for visual meteor observers", IMO 1995.

[9] A. Olech, M. Jurek, "1997 alpha-Aurigids from Poland", *WGN* 26 (1998), pp. 284–286.

[10] P. Jenniskens, "Meteor stream activity II. Meteor outbursts", *Astron. Astrophys.* 295 (1995), pp. 206–235.

[11] A. Dubietis, R.Arlt, "Thirteen years of Lyrids from 1988 to 2000", *WGN* 29 (2001), pp. 119–133.

[12] R. Arlt, "The analysis of a weak meteor shower: the June Bootids in 2000", *WGN* 28 (2000), pp. 98–108.

[13] J. Zvolankova, "Dependence of the observed rate of meteors on the zenith distance of the radiant", *Bull. Astron. Inst. Czechosl.* 34 (1983), pp. 122–128.

[14] L. Bellot Rubio, "Effects of a dependence of meteor brightness on the entry angle", *Astron. Astrophys.* 301 (1995), pp. 602–608.

Authors' addresses:

Audrius Dubietis, Baltupio 101-2, LT-2057 Vilnius, Lithuania, `audrius.dubietis@ff.vu.lt`.

Rainer Arlt, Friedenstr. 5, D-14109 Berlin, Germany, `rarlt@aip.de`.

Determination and Analysis of the New ι-Aurigid Meteor Shower from 1998, 1999, and 2000 Plotting Data

Huan Meng

Upon reviewing visual meteor plots of my Leonid observations of the last three years, a possible new shower with a radiant in Auriga was detected. Initially, the radiant was derived from 36 plotted meteors which diverged from it. The coordinates of the radiant were $\alpha = 76° \pm 5°$ and $\delta = +36° \pm 5°$ (for $\lambda_\odot = 235°$). It was found from the literature that Koschny and Zender derived the same new radiant from video observations of the 1998 Leonids. From available observations, some parameters of the new shower were derived, including the zenithal hourly rate, the population index, and the geocentric velocity. A population index of $r = 2.4 \pm 1.0$ was determined. A maximum ZHR of 14.5 ± 10.9 occurred at solar longitude $\lambda_\odot = 235°.465$ (November 17, 12^h37^m UT, 2000), and the meteor shower is active between $\lambda_\odot = 230°$ and $\lambda_\odot = 240°$. These parameters were derived from a quite limited number of data. In addition, a geocentric velocity $V_g = 46$ km/s was determined from video data.

1. Introduction

From 1998 onward, a group of meteor observers including myself have observed Leonids by the visual plotting method. During the 2000 Leonids, many meteors from different meteor streams of the northern sky were noticed. As soon as I came back from my observing site, I checked my Leonid observations from the previous years and found a possible new radiant. After that, many meteor plottings from that radiant were collected.

In Table 1, the observers whose full names are given do not have an *IMO* code. The T&A includes the Northern and Southern Taurids, and the α-Monocerotids; furthermore, the Leonids (LEO) and the ι-Aurigids (IAU) are distinguished; all other meteors are classified as sporadics.

Table 1 – Summary of the observations. Please refer to the text for more explanations.

Year	Date	Observer	T_{eff}	Lm	LEO	IAU	T&A	SPO
1998	November 13-14	SONWA	1.47	+5.8	0	0	2	3
1998	November 14-15	SONWA	3.90	+5.2	4	4	5	3
1998	November 16-17	MENHU	6.40	+5.3	88	16	40	33
1998	November 21-22	SONWA	2.44	+5.6	3	3	6	2
1999	November 11-12	SUNHU	1.99	+4.5	0	0	0	2
1999	November 15-16	SUNHA	4.84	+4.0	8	6	4	6
1999	November 17-18	MENHU	4.39	+5.2	43	6	12	13
1999	November 17-18	Gong Xuefei	2.10	+5.3	16	7	7	3
1999	November 17-18	SONWA	2.40	+4.9	5	3	4	2
1999	November 17-18	Ning Sixiaoxiao	3.80	+5.2	33	6	9	11
1999	November 19-20	SONWA	1.46	+4.9	1	1	3	1
2000	November 17-18	MENHU	1.08	+5.5		3	6	7
2000	November 20-21	SONWA	3.22	+5.4	3	4	5	4

2. Determination of the shower

In the work below, we used all the plots with limiting magnitude better than +4.0. Because of lack of time, I made the analysis quite early, so I did not include in it all the data collected later. All collected data are listed in Table 1.

The method that was used in the RADIANT program to search for the new shower was tracing. The method of tracing was simple, since the effect of the geocentric velocity on the position of the radiant was out of our consideration. We will come back to this in detail in Section 4.

A total of 196 meteors, most of which were initially classified as sporadics, were traced by this means. From these 196 meteors, there were 36 meteors with trails diverging from a narrow area in Auriga. The coordinates of the radiant obtained from this analysis are $\alpha = 76° \pm 5°$ and $\delta = +36° \pm 5°$ (for $\lambda_\odot = 235°$).

Also Koschny and Zender had mentioned that there might be a new radiant in Auriga from their Leonid video observations of 1998 [1]. The coordinates of that radiant on November 17, 1998 are $\alpha = 77° \pm 1°$ and $\delta = +35° \pm 2°$.

If we compare this radiant position with ours derived from meteor plots, we find them in very good agreement!

3. Analysis of the activity

Population index

In this work, we used the regression-line method—which uses the magnitude distribution—to determine the population index. We used an average value instead of the population index's profile.

It was considered that clustering data points could avoid large error margins. To lower the error margins in the situation like this is very important, so we used the data from all three years to determine one value. When considering the probabilities of perception, we referred to [2,3]. The value obtained is $r = 2.4 \pm 1.0$. We used this r-value for all calculations mentioned below.

The Zenithal Hourly Rate

The zenithal hourly rate (ZHR) is defined as in [4]:

$$\mathrm{ZHR} = \frac{r^{6.5-\mathrm{lm}} F}{\sin h_R} \times \frac{n}{T_{\mathrm{eff}}}, \tag{1}$$

where n is the number of shower meteors seen, r the population index, lm the limiting magnitude, F the field obstruction correction factor, T_{eff} the effective observing time in hours, and h_R the radiant elevation.

Figure 1 shows the composite ZHR profile of the ι-Aurigids from the years 1998, 1999, and 2000. We see that the activity level of the meteor shower varied smoothly. The maximum ZHR value was observed in 2000 at $\lambda_\odot = 235°.465$ with $\mathrm{ZHR}_{\mathrm{max}} = 14.5 \pm 10.9$. In that observation, the large error margin is caused by the large zenithal distance of the radiant.

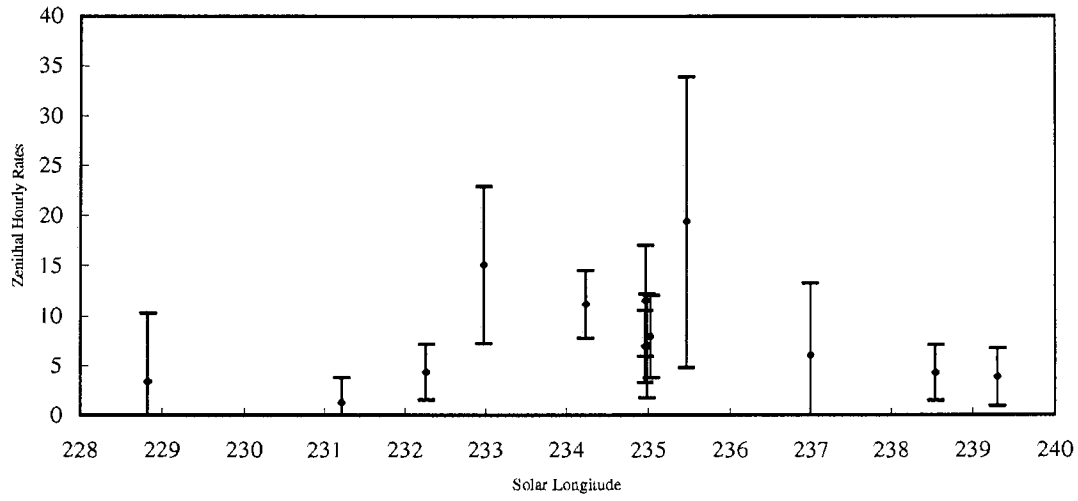

Figure 1 – The composite ZHR profile of the ι-Aurigids from the years 1998, 1999 and 2000.

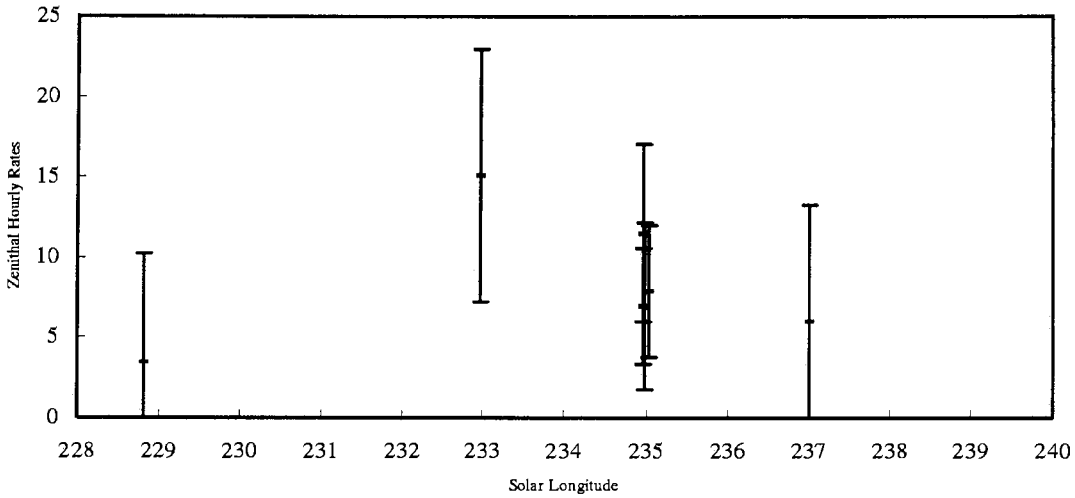

Figure 2 – The independent ZHR profile of the 1999 ι-Aurigids.

In Figure 2, we present a separate activity analysis of the ι-Aurigids in 1999, because of the large number of our plots from that year. There is a cluster of observational periods around $\lambda_{\odot} = 234.^{\circ}978$, which is shown in more detail in Figure 3. An average ZHR at that longitude is obtained by equation 2 below, as described in [4]:

$$\overline{\mathrm{ZHR}} = 1 + \frac{\sum_i n_i}{\sum_i T_{\mathrm{eff}}, i/C_i}, \tag{2}$$

where C is a factor of the observational conditions and the population index, other factors were all as mentioned as above.

The average ZHR for the four observations in Figure 4 is 7.3 ± 1.8.

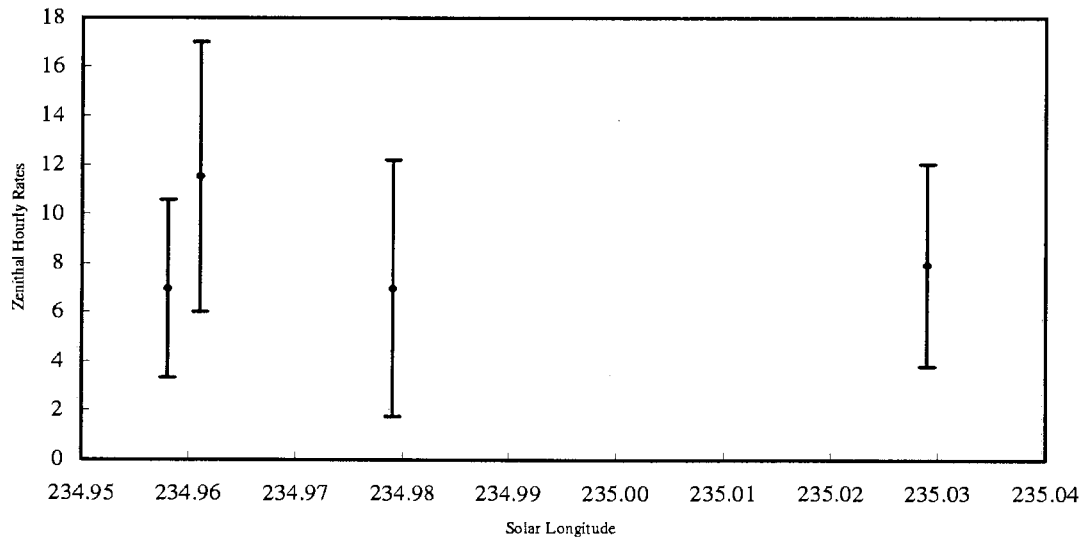

Figure 3 – A detail of the ZHR profile of the 1999 ι-Aurigids.

4. Discussion

Some parameters of this meteor shower still could not be determined from visual plotting observations only, e.g. the geocentric velocity. To confirm the existence of the shower, other methods can also be used. Therefore, we checked the video data provided by the *International Meteor Organization*, and found the radiant of the shower at very similar coordinates.

This data were also used to determine the geocentric velocity of the shower. We obtained it by the RADIANT 1.43 software [5]. At first we had determined the position of the radiant without considering the velocity, and we found out that the majority of the video data shows out the radiant. Thus, during this work, we checked different values of the velocity, and looked for the value that would give the most similar radiant. By this method, we checked all the available video data, and finally found $V_g = 46$ km/s, which corresponded the most to the position of the radiant.

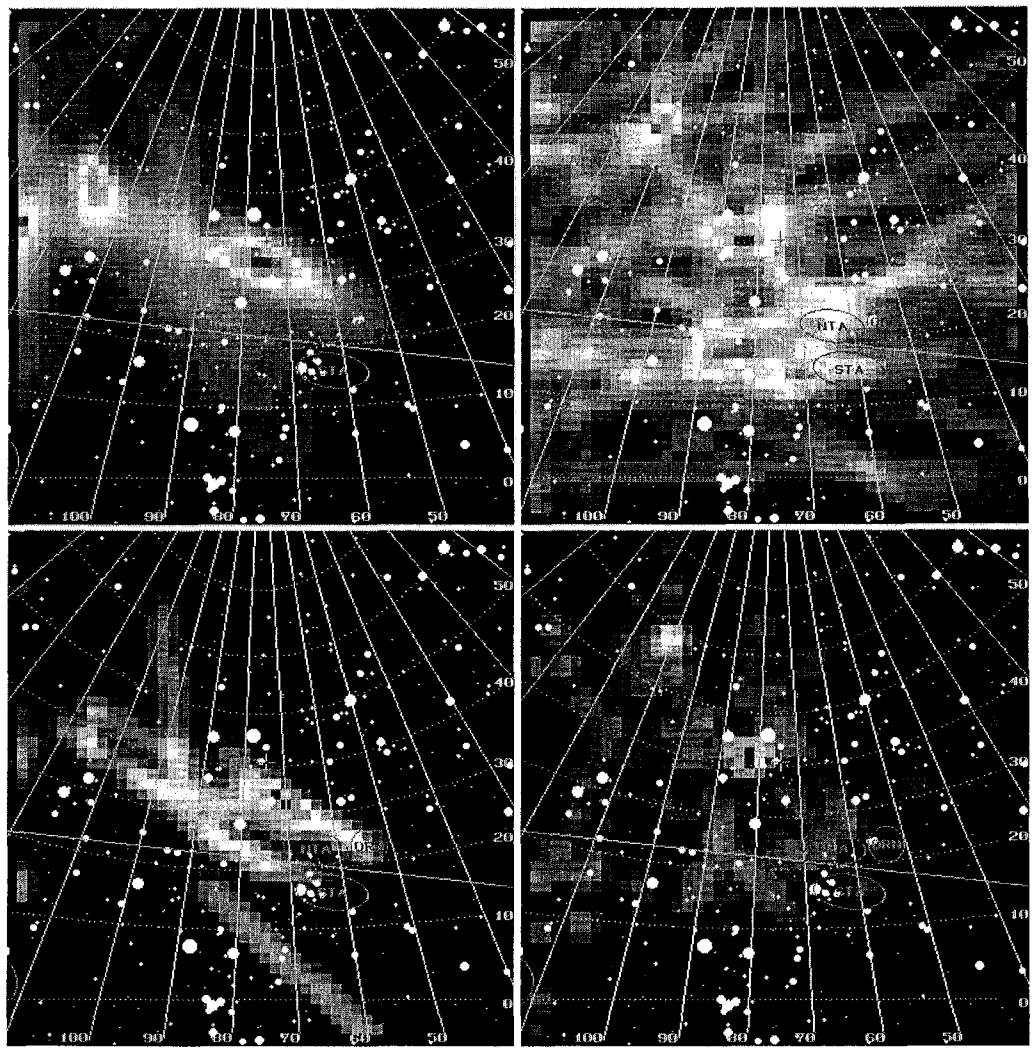

Figure 4 – The radiant of the ι-Aurigids obtained with the RADIANT software using video observations from two stations. A geocentric velocity of 46 km/s was obtained. For more details, please refer to the text

In Figure 4, the *top left* and *bottom right* pictures represent the analysis made by the "probabilities" and "intersections" methods, respectively, the other two represent the analysis made by the "tracings" methods. The *bottom left* and *top right* picture represent pairs of the double stations.

On the other hand, we tried to find the parent body of the ι-Aurigid meteor shower. No known minor body corresponded perfectly with this meteor shower. In spite of this the Comet C/LINEAR 2000 WM1 caught our attention. By the program described in [6] we computed: the radiant, the geocentric velocity and some other parameters. They are shown in Table 2.

Table 2 – The comet C/LINEAR 2000 WM1 parameters computed for the year 1999 (equinox 2000.0) by the software from [6].

Method	α	δ	V_g	V_H	Sol. Long.	Maximum	D-crit.
−Q	94.1	58.6	46.62	42.38	237.9	Nov 20.2	0.120
−B	95.6	59.2	45.94	41.63	237.9	Nov 20.2	0.115
−W	98.0	64.6	45.94	42.38	237.9	Nov 20.2	0.242
−A	162.4	52.7	46.38	42.48	283.3	Jan 3.7	0.738
−H	104.8	64.3	45.81	42.40	242.2	Nov 24.4	0.232
−P	96.6	61.9	45.41	42.39	240.1	Nov 22.3	0.143
Q+	36.6	−29.7	45.26	41.88	57.9	May 18.8	0.010
B+	36.6	−29.6	45.30	41.92	57.9	May 18.8	0.010
W+	36.5	−29.1	45.31	41.88	57.9	May 18.8	0.020
A+	39.9	−27.8	45.17	41.87	61.9	May 23.0	0.067
H+	36.8	−29.0	45.31	41.88	58.3	May 19.2	0.020
P+	36.6	−29.4	45.33	41.88	58.1	May 19.0	0.011

The parameters −Q and −B of the program [6] gave a perfectly corresponding geocentric velocity, and the position of the radiant was also similar to our position. The connection between this comet and the ι-Aurigids is doubtful, because this is a long period comet, and there was a difference in solar longitude of 2° between the date of the maximum computed and the observed one. When we observed meteors of this shower in the 1998, this LINEAR Comet was at a distance of 11.138 AU from the Earth, 11.650 AU from the Sun; and the Earth was 1116.5 days earlier to the comet in the node.

We are looking forward to obtaining the orbital elements of some ι-Aurigids from the video or the photographic multi-station observations. This elements could give us the relation between the new meteor shower and its parent body.

5. Conclusions

From our work and the literature [1], we are quite confident to confirm the existence of this new meteor shower and we can give some parameters of it.

The position of the radiant from our plots is $\alpha = 76.^\circ5$, $\delta = +36.^\circ5$; the population index is $r = 2.4 \pm 1.0$; the solar longitude of the peaks is usually between $\lambda_\odot$=233° and $\lambda_\odot = 236°$; the zenithal hourly rate at the maximum is 14.5 ± 10.9; the activity period is generally between $\lambda_\odot = 230°$ and $\lambda_\odot = 240°$, i.e. November 13 and November 22. The geocentric velocity was finally determined from the video data at 46 km/s.

No relation between the meteoroid stream and the known minor bodies can be determined. One possibility, which at this moment can not be confirmed, is the Comet C/2000 WM1.

There is a lot of video observations during the Leonids every year, therefore we can get from that data set a lot of information about other meteor showers active in that period, too. More work will be significant for the confirmation of the ι-Aurigids.

Acknowledgments

I thank J. Zhu especially for reviewing this article.

I'm also very grateful for the help to the next people: G. J. Wu, M. Davis, P. Wang, P. X. Xu, R. Arlt, S. Molau and Y. Qian;

To following visual plotting observers: H. M. Sun, S. X. X. Ning, W. F. Song and X. F. Gong;

And to the video observers: S. Molau and U. Sperberg.

Also, I would like to express my thanks for the support from the *National Natural Science Foundation of China* (Grant No. 10073012) for several meteor observations of mine in the *Xinglong Station* of the *National Astronomical Observatories of China (NAOC)*, including the 2000 Leonids.

References

[1] D. Koschny, J. Zender, "Possible New Radiant in Auriga on November 17, 1998", *WGN* 27:1, 1999, pp. 51–52.

[2] R. Koschack, J. Rendtel, "Determination of Spatial Number Density and Mass Index from Visual Meteor Observations (II)", *WGN* 18:4, 1990, pp. 119–140.

[3] R. Koschack, J. Rendtel, "Determination of Spatial Number Density and Mass Index from Visual Meteor Observations (I)", *WGN* 18:2, 1990, pp. 44–58.

[4] R. Arlt, "The Analysis of a Weak Meteor Shower: The June Bootids in 2000", *WGN* 28:4, 2000, pp. 98–108.

[5] R. Arlt, "The Software RADIANT", *WGN* 20:2, 1992, pp. 62–69.

[6] L. Neslušan, J. Svoreň, V. Porubčan, "A Computer Program for Calculation of a Theoretical Meteor-Stream Radiant", *Astron. Astrophys.* 331, 1998, pp. 411–413.

Authors' address

Huan Meng, Beijing No.80 Middle School, Beijing 100020, China

SPA Meteor Section Results: March–April 2001

Alastair McBeath

News and reports reaching the *SPA Meteor Section* from 2001 March and April are given. March was a month of vague meteoric events in the UK, including a meteorite fall that wasn't on March 1 and possibly several bright fireballs on March 13-14, such interest perhaps engendered by the expected atmospheric re-entry of the Mir space station, which came down over the southern Pacific Ocean on March 23. A fireball seen from six sites across southern England happened at 20^h40^m UT on April 10-11. Moon-free conditions for the Lyrid maximum later in April allowed some useful coverage, but the peak could not be clearly defined on April 21-22. The radio results loosely favoured a maximum between $7^h - 10^h$ UT on April 22, centered around $8^h30^m \pm 1^h$ UT ($\lambda_\odot(eq.\ J2000.0) = 32°.2 - 32°.33$ and $32°.26 \pm 0°.04$ respectively), though unusual radio peaks were also found in some datasets on April 20 and 21, but with little consensus in timing between observers on these earlier dates.

1. Introduction

As in 2000, March was a quiet month for visual observations, as February's poor weather dragged on into the northern early spring. April saw more observer activity generally, chiefly from the Section's correspondents outside the British Isles. Table 1 has the observing totals.

Radio results, except those sent in by Dirk Artoos, were extracted from *Radio Meteor Observation Bulletins* 92, 93 and 95, dated March, April and June 2001 respectively, kindly provided by Chris Steyaert.

The radio observers were:

> Enric Fraile Algeciras (Spain), Dirk Artoos (Belgium), Mike Boschat (Nova Scotia, Canada), Gabor Bucsi (Hungary), Patrick Decomble (France), Maurice de Meyere (Belgium), Ghent University (Belgium), Will Kelsey (Arkansas, USA), Stan Nelson (New Mexico, USA), Hiroshi Ogawa (Japan), Sadao Okamoto (Japan), Dave Swan (England), Istvan Tepliczky (Hungary), Pierre Terrier (France), Ouyang Tianjing (China), Garfield Tsao (Taiwan), Bruce Young (Queensland, Australia), Ilkka Yrjölä (Finland)

The raw data were analyzed as normal (see [1]), and Figure 1 shows a representative dataset from both months.

Video data came primarily from monthly summaries produced by the German *Arbeitskreis Meteore (AKM)* group. These summaries are among the *IMO-News* e-mailing list notices, but with the other AKM results used here, more complete versions have been taken from their monthly journal *Meteoros*, 4:4-5 and 4:6 (2001), sent in by Ina Rendtel.

The observers reporting were (in Germany where not noted):

> Orlando Benitez-Sanchez (Canary Isles), Steve Evans (England), Detlef Koschny (Netherlands), André Knöfel, Rob McNaught (New South Wales, Australia), Sirko Molau, Mirko Nitschke, Jürgen Rendtel, Jörg Strunk, Ilkka Yrjölä (Finland)

Our visual observers included:

> *American Meteor Society (AMS)* reporters Mark Davis, George Gliba, Robert Hayes, Carl Johannink (Germany and Netherlands), Pierre Martin (Ontario, Canada), Roger Venable (all in the USA where not noted; based on data summaries in the *AMS* journal *Meteor Trails* 11 and 12 (June and September 2001 respectively) thoughtfully submitted by Bob Lunsford); AKM members Rainer Arlt, Darja Golikowa, Ralf Kuschnik, Hartwig Lüthen, Sven Näther, Jürgen Rendtel, Roland Winkler, Oliver Wusk (all in Germany except Oliver Wusk, who was in Queensland, Australia); Phil Heppenstall (England), Marco Langbroek (Netherlands), Bob Lunsford (California, USA), Alastair McBeath (England)

2. March

March in the UK began with what was suggested initially as a meteorite fall near York on the morning of March 1. Excited news reports mentioned the fall being accompanied by a loud bang and a rush of air as it narrowly missed a woman out walking her dog in the early morning, and leaving a smoking crater in the earth making popping and cracking noises. Of course, this all set cautionary alarm bells ringing in the minds of those who have studied such events before, as being highly improbable with a small natural meteorite fall, though this did not stop one curator from the *Yorkshire Museum* from claiming it as a definite meteorite fall, despite the lack of evidence! The first pictures of the crater were available by early afternoon, and showed a very odd shape: a hole around 1 m deep by around 25 cm outer diameter, tapering narrower in a tubular cone deeper into the ground. By mid-afternoon, the truth was revealed by a military bomb disposal team. No meteorite, only a short-circuiting underground electricity cable, which had exploded and hurled clods of earth into the air, fizzing and smoking once the air could get to it!

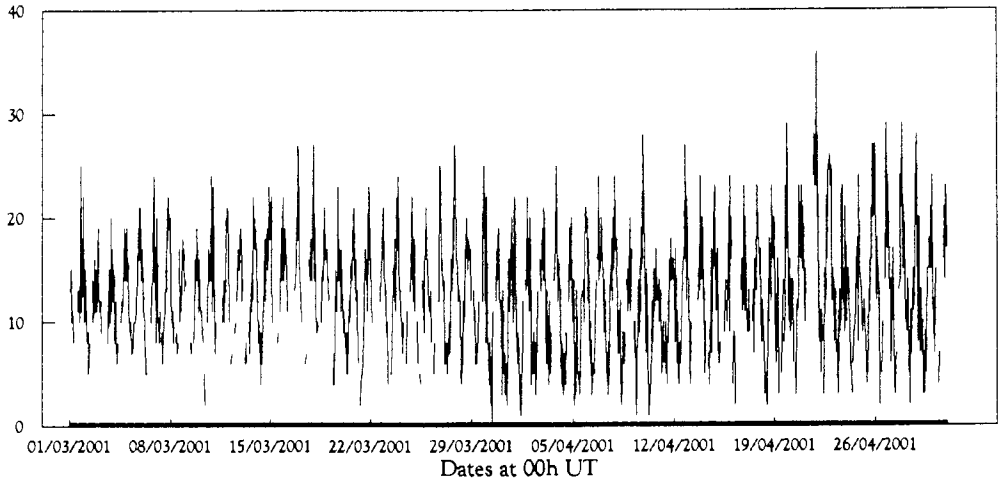

Figure 1 – Raw hourly all-echo radio meteor counts from 2001 March and April, in data collected by Hiroshi Ogawa. Hiroshi's set-up was operated continuously, but appears somewhat fragmentary in places due to almost daily interference problems, a difficulty all the Japanese radio observers have found in recent times, especially during the local afternoon hours. The Lyrids produced a clear peak in April, with enhanced rates towards late April most likely due to pre-peak η-Aquarid activity.

The minor radio peaks from [1] were mostly recovered as previously, with little variance from earlier years. The $\lambda_\odot = 346° - 347°$ (March 7-8) and 350° (March 11) minor maxima were not well-seen however, though $\lambda_\odot = 348°$ did produce something in 56% of the available datasets. The $\lambda_\odot = 350°$ peak seemed spread across $\lambda_\odot \approx 349° - 352°$ in several reports, as has been found before. The $\lambda_\odot = 359° - 4°$ peak (March 20-25) showed notable, if slight, maxima at $\lambda_\odot = 1° - 2°$ in all the available results, plus at $\lambda_\odot = 359°$ and $4° - 5°$ in 2/3 of the datasets, the $1° - 2°$ spell especially being better recorded than previously. The extended $\lambda_\odot = 7° - 8°$ peak (sometimes running between around $6° - 11°$, March 27 to April 1) was fairly ill-defined as normal, although with a good consensus in all-but one dataset for a small peak at 11° for once.

On March 13-14, several media sources reported on one or more fireballs during the UK evening hours apparently occurring over the English Channel off the south or south-east coasts of England. Two fireball reports, one from England around 18^h50^m UT, the other from Germany at 19^h50^m UT, were forwarded by Section correspondents, but no other eye-witness sightings were secured despite follow-up notices in various places.

A final "media fireball" for March happened on March 23, when the Mir space station re-entered the Earth's atmosphere and burnt up high above the southern Pacific Ocean east of New Zealand. TV and press coverage of the final moments of the burn-up was extensive and spectacular, plus for anyone involved in meteorite recovery or advising observers about typical natural and man-made meteoric appearances, invaluable, showing just how extremely slowly man-made meteors seem to track across the heavens!

3. April

The early April minor radio maxima were all detected by most observers, the $\lambda_\odot = 13°/14° - 19°$ period (April 3/4 to 9) as ill-defined as usual, while the $\lambda_\odot = 22° - 24°$ peak, best at $\lambda_\odot \approx 23° - 24°$ this year (April 13-14), was better confirmed than in 1999–2000. No clear consensus was apparent regarding when the $\lambda_\odot = 25° - 28°$ (the extended $25° - 27°$ spell; April 15-18) peaked however, but it showed less sign of blending into the previous peak than in some past years.

April 10-11, 20^h40^m UT, brought a fireball event reported by six observers spread across southern England from Surrey and Bedfordshire west to Dorset and Somerset, who were out to spot the International Space Station (ISS), which was just finishing its evening pass as the fireball took place. Most of the reports indicate the fireball fragmented late in its flight, reaching about magnitude -4 at best. The ISS distraction meant few people could give even a rough estimate for the sky position, but the object was probably out over the western Channel, perhaps heading from above south Devon towards the Cotentin Peninsula of northern France on an approximately north-west (perhaps north-north-west) to south-east (or south-south-east) track.

The moonless Lyrids were eagerly anticipated, though the British weather failed to cooperate, and most observers here recorded only cloudy skies nearest the shower's predicted best. Elsewhere, circumstances were significantly better, and useful datasets are available from Germany and the USA especially. Even these did not provide ideal coverage across the maximum this year, since as noted in the preliminary *IMO* report [2], the Lyrid peak seemed rather plateau-like for about a day, probably from before about 18^h UT on April 21 to after 21^h30^m UT on April 22. ZHRs in our results were around 25 ± 5 for most of the night on April 21-22 over Europe and North America, and without a clear, single maximum certainly. Too few magnitude and train distribution details were received for an analysis of these unfortunately.

Twelve radio observers provided enough comparison data around the Lyrid maximum to try to better define the radio peak. A careful examination of these results loosely favoured a maximum between $7^h - 10^h$ UT on April 22, centered most probably around $8^h30^m \pm 1^h$ UT ($\lambda_\odot = 32\overset{\circ}{.}2 - 32\overset{\circ}{.}33$, and $32\overset{\circ}{.}26 \pm 0\overset{\circ}{.}04$ respectively), though several reports favour almost comparably strong activity on both April 21-22 and 22-23. Unusual, sometimes quite strong, radio peaks were also found in a few datasets on April 20 (two only) and 21, but there was little consensus in the timing of these events between observers on these earlier dates. Some of these unusual events may have been due to unidentified interference, perhaps early Sporadic-E, or possibly unexpected higher Lyrid activity, but this is unknown. There is little support that any of the activity around the expected Lyrid peak was due to stronger rates from the π-Puppids at least. Overall though, there is support in the radio data for the preliminary visual Lyrid results in finding a very ill-defined and probably quite long-lasting Lyrid maximum in 2001. The main radio peak being better delineated might hint at somewhat stronger than normal activity, but this cannot be inferred from the available information. The radio peak fell close to the time of higher-rate Lyrid returns from 1988–2000 however ($\lambda_\odot = 32\overset{\circ}{.}32$ [3]).

After the Lyrids, minor radio peaks were found around $\lambda_\odot \approx 37° - 39°$ especially, in the $\lambda_\odot = 34° - 39°$ period (April 24-29), while $\lambda_\odot = 40° - 41°$ showed the main maxima in the extended $\lambda_\odot = 40°$ spell ($\lambda_\odot = 39° - 41°$, April 29 to May 1), in the run-up towards the best from the early May η-Aquarids.

Table 1 – Visual, radio and video hours' totals, with visual and video meteor numbers recorded in each month, including a partial breakdown of visual meteor types.

Month	Visual	VIR	LYR	SAG	Meteors	Radio	Video	Video met
March	$14^h.0$	11	–	–	102	7058^h	$366^h.4$	3075
April	$75^h.6$	9	271	19	689	7977^h	$455^h.7$	3744

Acknowledgments

My final pleasant duty is as always to thank all the *Section's* contributing observers and correspondents from these two months. Clear skies!

References

[1] A. McBeath, "The Forward Scatter Meteor Year: 2001 Update", *WGN* 29:3, 2001, pp. 85–92.

[2] R. Arlt, V. Krumov, "IMO Shower Circular: Lyrids 2001", *on IMO-News e-mail list*, 24 April 2001.

[3] A. Dubietis, R. Arlt, "Thirteen Years of Lyrids from 1988–2000", *WGN* 29:4, 2001, pp. 119–133.

SPA Meteor Section Results: May–June 2001

Alastair McBeath

Results and information collected by the *SPA Meteor Section* from 2001 May and June is presented and discussed. The moonlit η-Aquarid maximum in early May was poorly-observed visually, and somewhat ill-defined in the radio results, but with a general consensus for a stronger peak around May 5-6, much as expected, perhaps with a tail of increased activity persisting for a further two days after this. No trace of any visual meteors associated with Comet 73P/Schwassmann-Wachmann 3 (SW3) was found, although the minor radio peak detected previously at $\lambda_\odot$ (eq. J2000.0) = 68° – 70° did produce a small maximum around $\lambda_\odot \approx 70°$, May 31, in all available datasets. This is unlikely to have been due to unusual SW3 meteor rates however. There was also little trace of June Lyrid or June Bootid activity either in the visual or radio data from June, the radio activity not assisted by another strong Sporadic-E season.

1. Introduction

May and June turned out to be months more memorable for what was not seen than what was, though observations confirming no obvious meteor activity can be just as valuable as witnessing new or unexpected meteor showers of course, even if not as interesting! Twilight overnight in the northern hemisphere was a further deterrent for visual watchers, plus Sporadic-E (Es) was again very problematical for our radio workers. Regrettably, several radio observers were unable to provide information on when Es created difficulties this year, and in order to maintain a reasonable standard of analysis, all those observations without any reference to interference problems after mid-May and in June were omitted from further study. I would again urge all radio observers to please try to identify such problems in their reports in future. The loss of data because of this information lack was over 1300 hours in May, and over 2500 hours in June. The totals in Table 1 do not include these "missing" data.

Dirk Artoos provided his radio results directly, while the remaining radio reports were sent in by Chris Steyaert as *Radio Meteor Observation Bulletins* 94–96 inclusive, May to July 2001.

The radio observers were:

Enric Fraile Algeciras (Spain), Dirk Artoos (Belgium), Mike Boschat (Nova Scotia, Canada), Patrick Decomble (France), Maurice de Meyere (Belgium), Ghent University (Belgium), Will Kelsey (Arkansas, USA), Marc Le Foll (France), Stan Nelson (New Mexico, USA), Hiroshi Ogawa (Japan), Sadao Okamoto (Japan), Ton Schoenmaker (Netherlands), Dave Swan (England), Istvan Tepliczky (Hungary), Pierre Terrier (France), Ouyang Tianjing (China), Garfield Tsao (Taiwan), Bruce Young (Queensland, Australia), Ilkka Yrjölä (Finland)

The normal analysis were carried out on these, as detailed in [1], and a graph showing representative results is given here as Figure 1.

The video observations came exclusively from the monthly summaries of the German *Arbeitskreis Meteore (AKM)* group. Along with the other *AKM* results used here, these were extracted from their monthly journal *Meteoros*, 4:6 and 4:7 (2001), submitted by Ina Rendtel.

The observers were (in Germany if not stated):

Orlando Benitez-Sanchez (Canary Isles), Steve Evans (England), Detlef Koschny (Netherlands), André Knöfel, Rob McNaught (New South Wales, Australia), Sirko Molau, Mirko Nitschke, Jürgen Rendtel, Jörg Strunk, Ilkka Yrjölä (Finland)

Visual reports were received from:

American Meteor Society (AMS) members (in the USA where not noted; taken from summaries in the *AMS* journal *Meteor Trails* 12 (September 2001) provided by Bob Lunsford) Mark Davis, Robin Gray, Carl Johannink (Germany and Netherlands), Catherine Kerg, Pierre Martin (Ontario, Canada), Paul Martsching, Kim Youmans; AKM members (in Germany if not mentioned) Frank Enzlein, Sven Näther, Jürgen Rendtel (Germany and Tenerife), Roland Winkler, Oliver Wusk (Queensland, Australia); Eva Bojurova (Bulgaria, including notes from the Astroclub Canopus η-Aquarid observations), Marco Langbroek (Netherlands), Bob Lunsford (California, USA), Alastair McBeath (England)

2. May

Moonlight was always going to be a problem for η-Aquarid observations near their early May maximum, and so it proved, though for our chiefly northern hemisphere visual watchers, the shower is always a difficult target with a radiant-rise close to the start of morning twilight anyway. More useful radio observing was possible across the expected maximum. The extended $\lambda_\odot = 40°$ minor peak from [1] ($\lambda_\odot = 39° - 41°$, April 29 to May 1) was picked up by most radio reporters, and during the $\lambda_\odot = 42° - 50°$ spell (May 2-11), the better consensus on a stronger peak was achieved in 78% of the recordings around $\lambda_\odot = 44° - 45°$ (May 5-6). A lesser consensus on other peaks within this spell was found around $\lambda_\odot = 46°$ (60% of datasets) and 47° (50%), May 7 and 8, which perhaps suggests a waning tail to the maximum activity predicted for May 5-6 [2]. The overall "bulge" in radio rates coincident with the η-Aquarids' best in early May is clear at least in all the radio results covering the first half of May, as Figure 1 demonstrates.

Regarding the other, minor, radio peaks in May, the $\lambda_\odot = 52° - 53°$ period (May 13-14) occurred in most datasets, but extended from $\lambda_\odot = 51°$ in some this year, while the $\lambda_\odot = 54° - 58°$ peak (May 15-19) was noted better around $\lambda_\odot = 55°$ and 57°, but without a clear consensus between observers. The $\lambda_\odot = 60° - 61°$ (May 21-22) spell, first found in 1998, was poorly detected in only half the datasets, though the $\lambda_\odot = 62° - 66°$ time (May 23-27) was seen more clearly than in 1998–2000, but without a clear agreement as to when during these five days the peak actually fell. Radio observations during the second half of May were hampered by increasing Es, as already mentioned.

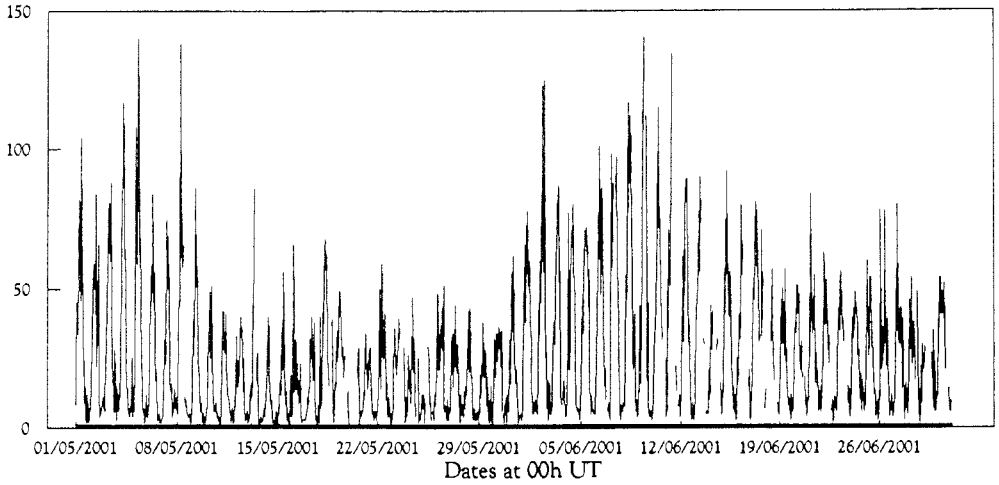

Figure 1 – Raw hourly radio meteor percentage reflection time echo counts (×10) from 2001 May and June as reported by Pierre de Groote of the University of Ghent. The system was run continuously, with the breaks due to interference problems, primarily Es, which was especially bad at times in June. The η-Aquarids gave the obvious peak in early May, while the Arietids and ζ-Perseids repeat the procedure in early June.

Following well-timed warnings about possible activity from a new radiant around 10° north of the bright star Arcturus in Bootes, associated with Comet 73P/Schwassmann-Wachmann 3 (SW3) in *WGN* [3] and on *IMO-News* on May 29, visual and radio observers reporting to us found no significant trace of SW3 meteor rates from this source, confirming the preliminary *IMO* report [4]. Although the minor radio peak found previously around $\lambda_{\odot} = 68° - 70°$ (May 29-31, the extended $\lambda_{\odot} = 69°$ period), was best at $\lambda_{\odot} \approx 70°$, it is very unlikely this was due to unusual SW3 meteor rates.

3. June

The northern twilight month of June provided opportunities to check on the possible June Lyrids and for any June Bootid activity with minimal lunar interference, but little trace of either source was found in the visual data. There were a few comments that some possible June Lyrid activity may have come instead from a very minor radiant in Draco, combined with some misidentified sporadics. Interestingly, most observers who noted some June Lyrids recorded similar, or stronger, Sagittarid activity during the proposed Lyrid epoch too, which given the southerly Declination of the Sagittarid radiant suggests that the Lyrid rates were exceptionally weak, if genuine at all.

The radio peaks in June from [1] were mostly recovered despite some strong Es interference again for our northern hemisphere reporters. The $\lambda_{\odot} = 71°$ peak (June 1) was found in all the available results, and was seen moderately strongly in half, unlike in 1998–2000, but the $\lambda_{\odot} = 73°$ peak (June 4) was not well-detected. Combined activity from the daytime Arietids and ζ-Perseids produced the usual $\lambda_{\odot} = 75° - 82°$ (June 6-13) "bulge" in radio rates, as Figure 1 nicely demonstrates, with the stronger peaks around $\lambda_{\odot} = 77°$ and 79° (June 8 and 10 respectively), in both cases about a day later than the maxima were expected based on earlier radar data, though these observed timings are perfectly in-line with radio results from more recent times. An earlier, lesser, peak was apparent around $\lambda_{\odot} = 74° - 75°$, as has been seen before, while the $\lambda_{\odot} = 79°$ peak seemed to have a tail of somewhat increased rates persisting through to $\lambda_{\odot} = 81°$ this year.

The $\lambda_\odot = 84°$ peak gave a clear response over its extended period this time, with minor maxima especially noted at $\lambda_\odot \approx 83°$ and $86° - 87°$ (June 14 and 17-18 respectively), and showed less tendency to blend in with the peaks preceding it than has been seen before. With no definite June Bootids featuring in the visual results in late month, it is unsurprising to find the stronger late June radio peaks more likely to be associated with the daytime β-Taurids than the Bootids, with the $\lambda_\odot = 89° - 97°$ spell producing two main peaks around $\lambda_\odot = 90°$ and 92° (June 21 and 23), the time the better rates from this source have been found sometimes during much of the last decade. A small peak was registered around $\lambda_\odot = 95° - 96°$ too (June 27-28), which might perhaps hint at some low Bootid rates, but as this minor peak has been found before in other years when visual June Bootid rates have been absent, this is not good evidence for the shower's presence in 2001.

Table 1 – Visual, radio and video hours' totals, visual and video meteor numbers recorded in each month, including a partial breakdown of meteor types.

Month	Visual	Meteors	SAG	ETA	Radio	Video	Trails
May	$54^h.5$	386	40	12	$6866^h.75$	$563^h.9$	4219
June	$112^h.1$	977	102	–	3922^h	438^h	6363

Acknowledgments

My grateful thanks go to all our observers and correspondents whose efforts make such reports as this possible. Clear skies for all your observing!

References

[1] A. McBeath, "The Forward Scatter Meteor Year: 2001 Update", *WGN* 29:3, 2001, pp. 85–92.

[2] A. McBeath, R. Arlt, "Meteor Shower Calendar: April–September 2001", *WGN* 29:1/2, 2001, pp. 5–10.

[3] H. Lüthen, R. Arlt, M. Jäger, "The Disintegrating Comet 73P/Schwassmann-Wachmann 3 and Its Meteors", *WGN* 29:1/2, 2001, pp. 15–28.

[4] R. Arlt, "IMO Shower Circular: No Activity from Comet Schwassmann-Wachmann 3 in 2001", *on IMO-News e-mail list*, 31 May 2001.

The International Meteor Organization

Council

President: Jürgen Rendtel, Seestraße 6, D-14476 Marquardt, *Germany*,
tel. +49 (33208) 50753, e-mail: president@imo.net

Vice-Pres.: Alastair McBeath, 12A Prior's Walk, Morpeth, Northumberld. NE61 2RF, *Engl.*,
tel. +44 (1670) 518 487, email: vice_president@imo.net

Secretary-General: Robert Lunsford, Vance Street 161, Chula Vista, *CA 91910, USA*
tel. +1 (619) 585 9642, e-mail secretary@imo.net

Treasurer: Ina Rendtel, Mehlbeerenweg 5, D-14469 Potsdam, *Germany*,
tel. +49 (331) 520 707, e-mail: treasurer@imo.net
postal (giro) account number: 5472 34-107
bank code: 100 100 10 Postbank Berlin
(bank code and postbank to be mentioned together with account number!)

Other council members:
Rainer Arlt, Friedenstraße 5, D-14109 Berlin, *Germany*
Marc Gyssens, Heerbaan 74, B-2530 Boechout, *Belgium*
André Knöfel, Saarbrücker Straße 8, D-40476 Düsseldorf, *Germany*
Sirko Molau, Weidenweg 1, D-52074 Aachen, *Germany*

Commission Directors

Visual Commission: Rainer Arlt, e-mail: visual@imo.net

Telescopic Commission: M. Currie, 660, N'Aohoku Place, Hilo, *HI 96720, USA*,
e-mail: tele@imo.net

FIreball DAta Center: André Knöfel, e-mail: fidac@imo.net

Photographic Commission: Marc de Lignie, Prins Hendrikplein 42, NL-2264 SN Leidschendam,
the Netherlands, e-mail: photo@imo.net

Video Commission: Sirko Molau, e-mail: video@imo.net

Radio Commission: vacant, e-mail: radio@imo.net

WGN — The Journal of the International Meteor Organization and Observational Report Series

Editor-in-chief: Marc Gyssens, tel. 32 (477) 64 05 48, e-mail: wgn@imo.net
fax: 32 (11) 26 82 99 (mention "for Marc Gyssens")

Editorial board: R. Arlt, D. Asher, M. Beech, P. Brown, M. Currie, M. de Lignie, W. Elford, G. Kronk, R. Hawkes, D. Hughes, J. Jones, C. Keay, R. Koschack, A. McBeath, D. Meisel, P. Pravec, J. Rendtel, M. Šimek, G. Spalding, I. Williams.

Typesetting: Urania, the Public Observatory of Antwerp

Web Site: http://www.imo.net

Do not miss it!

International Meteor Conference 2002

Frombork, Poland, September 26–29, 2002

Do not miss this unique opportunity to meet like-minded people! We anticipate that a lot of meteor enthusiasts from all over Europe and overseas will participate. Results on the 2001 Leonids and discussions on the 2002 Leonids may be expected. More information can be found on page 1 of this issue of our Journal!

The stock of the IMO

	EUR	USD
Publications in English:		
Photographic Meteor Data Base (1986)	4	4
Proceedings International Meteor Conference 1990	5	5
Proceedings International Meteor Conference 1991	5	5
Proceedings International Meteor Conference 1992	5	5
Proceedings International Meteor Conference 1993	5	5
Proceedings International Meteor Conference 1994	5	5
Proceedings International Meteor Conference 1995	5	5
Proceedings International Meteor Conference 1996	5	5
Proceedings International Meteor Conference 1998	6	6
Proceedings International Meteor Conference 1999	6	6
Proceedings International Meteor Conference 2000	6	6
Gnomonic Atlas Brno 2000.0	3	3
Photographic Astrometry + diskette	7	7
WGN Observational Report Series:		
Vols. 1–5 (1988–1992): Visual Observations, per vol.	8	8
Vol. 6 (1993): Vis. Obs. and Electrophonic Fireball Cat.	8	8
Vols. 7–8 (1994–1995): Visual Observations, per vol.	8	8
Vols. 9–12 (1996–1999): Visual Observations, per vol.	10	10
Backissues of the WGN Journal:		
Volumes 19–20 (1991–1994): complete, per volume:	10	10
Volumes 23–29 (1995–2001): complete, per volume:	18	18